Impact of Seasonal Hypoxia on Activity and Community Structure of Chemolithoautotrophic Bacteria in a Coastal Sediment

Yvonne A. Lipsewers,*[a] Diana Vasquez-Cardenas,*[a] Dorina Seitaj,[a] Regina Schauer,[b] Silvia Hidalgo Martinez,[a] Jaap S. Sinninghe Damsté,[a, c] Filip J.R. Meysman,[a, b, d] Laura Villanueva,[a] Henricus T.S. Boschker,[a]

*equal contributors

Departments of Marine Microbiology and Biogeochemistry, and Estuarine and Delta Systems, NIOZ Royal Netherlands Institute for Sea Research, Texel and Utrecht University, The Netherlands,[a]; Department of Bioscience, Microbiology, Aarhus University, Aarhus, Denmark,[b]; Utrecht University, Faculty of Geosciences, Department of Earth Sciences, Utrecht, The Netherlands,[c]; Vrije Universiteit Brussel (VUB), Department of Environmental, Analytical and Geo-Chemistry, Brussels, Belgium,[d]

Running title: Chemolithoautotrophy in seasonally hypoxic sediments

Corresponding authors: eric.boschker@nioz.nl; laura.villanueva@nioz.nl

This article has been published in *Applied and Environmental Microbiology*, 83:e03517-16. https://doi.org/10.1128/AEM.03517-16.

ABSTRACT

Seasonal hypoxia in coastal systems drastically changes the availability of electron acceptors in bottom water, which alters the sedimentary reoxidation of reduced compounds. However, the effect of seasonal hypoxia on the chemolithoautotrophic community that catalyze these reoxidation reactions, is rarely studied. Here we examine the changes in activity and structure of the sedimentary chemolithoautotrophic bacterial community of a seasonally hypoxic saline basin under oxic (spring) and hypoxic (summer) conditions. Combined 16S rRNA gene amplicon sequencing and analysis of phospholipid derived fatty acids indicated a major temporal shift in community structure. Aerobic sulfur-oxidizing Gammaproteobacteria (Thiotrichales) and Epsilonproteobacteria (Campylobacterales) were prevalent during spring, whereas Deltaproteobacteria (Desulfobacterales) related to sulfate reducing bacteria prevailed during summer hypoxia. Chemolithoautotrophy rates in the surface sediment were three times higher in spring compared to summer. The depth distribution of chemolithoautotrophy was linked to the distinct sulfur oxidation mechanisms identified through microsensor profiling, *i.e.*, canonical sulfur oxidation, electrogenic sulfur oxidation by cable bacteria, and sulfide oxidation coupled to nitrate reduction by Beggiatoaceae. The metabolic diversity of the sulfur-oxidizing bacterial community suggests a complex niche partitioning within the sediment probably driven by the availability of reduced sulfur compounds (H_2S, S^0, $S_2O_3^{-2}$) and electron acceptors (O_2, NO_3^-) regulated by seasonal hypoxia.

IMPORTANCE

Chemolithoautotrophic microbes in the seafloor are dependent on electron acceptors like oxygen and nitrate that diffuse from the overlying water. Seasonal hypoxia however drastically changes the availability of these electron acceptors in the bottom water, and hence, one expects a strong impact of seasonal hypoxia on sedimentary chemolithoautotrophy. A multidisciplinary investigation of the sediments in a seasonally hypoxic coastal basin confirms this hypothesis. Our data show that bacterial community structure and the chemolithoautotrophic activity varied with the seasonal depletion of oxygen. Unexpectedly, the dark carbon fixation was also dependent on the dominant microbial pathway of sulfur oxidation occurring in the sediment (*i.e.*, canonical sulfur oxidation, electrogenic sulfur oxidation by cable bacteria, and sulfide oxidation coupled to nitrate reduction by Beggiatoaceae). These results suggest that a complex niche partitioning within the sulfur-oxidizing bacterial community additionally affects the chemolithoautotrophic community of seasonally hypoxic sediments.

INTRODUCTION

The reoxidation of reduced intermediates formed during anaerobic mineralization of organic matter is a key process in the biogeochemistry of coastal sediments (1, 2). Many of the microorganisms involved in the reoxidation of reduced compounds are chemolithoautotrophs, which fix inorganic carbon using the chemical energy derived from reoxidation reactions (dark CO_2 fixation). In coastal sediments, sulfate reduction forms the main respiration pathway, accounting for 50% to 90% of the organic matter mineralization (1). The reoxidation of the pool of reduced sulfur compounds produced during anaerobic mineralization (dissolved free sulfide, thiosulfate, elemental sulfur, iron monosulfides and pyrite) hence forms the most important pathway sustaining chemolithoautotrophy in coastal sediments (2, 3).

Various lineages from the Alpha-, Gamma-, Delta- and Epsilonproteobacteria, including recently identified groups, such as particle-associated Gammaproteobacteria and large sulfur bacteria, couple dark CO_2 fixation to the oxidation of reduced sulfur compounds in oxygen deficient marine waters and sediments, in coastal marine sediments and in lake sediments (4−9). Both chemolithoautotrophic sulfur-oxidizing Gammaproteobacteria and sulfur disproportionating Deltaproteobacteria have been identified to play a major role in the sulfur and carbon cycling in diverse intertidal sediments (10−12). Hence, chemolithoautotrophic sulfur-oxidizing communities vary between sediment environments, but it is presently not clear as to which environmental factors are actually determining the chemolithoautotrophic community composition at a given site.

Seasonal hypoxia is a natural phenomenon that occurs in coastal areas around the world (13) and provides an opportunity to study the environmental factors controlling sedimentary chemolithoautotrophy. Hypoxia occurs when bottom waters become depleted of oxygen (< 63 µmol O_2 L^{-1}), and has a large impact on the biogeochemical cycling and ecological functioning of the underlying sediments (13). The reduced availability or even absence of suitable soluble electron acceptors (O_2, NO_3^-) in the bottom water during part of the year should in principle result in a reduction or complete inhibition of sedimentary sulfur reoxidation, and hence, limit chemolithoautotrophy. At present, the prevalence and temporal variations of chemolithoautotrophy have not been investigated in coastal sediments of seasonal hypoxic basins.

Likely, the availability of soluble electron acceptors (O_2, NO_3^-) in the bottom water is not the only determining factor of chemolithoautotrophy. A recent study conducted in a seasonally hypoxic saline basin (Lake Grevelingen, The Netherlands) indicated that the intrinsic structure and composition of the sulfur oxidizing microbial community also determined the biogeochemistry of the sediment (14). In this study, three distinct microbial sulfur oxidation mechanisms were observed throughout a seasonal cycle: (1) electrogenic sulfur oxidation by heterotrophic cable bacteria (Desulfobulbaceae); (2) canonical aerobic oxidation of free sulfide at the oxygen-sulfide interface and, (3) sulfide oxidation coupled to nitrate reduction by filamentous members of the Beggiatoaceae family that store nitrate intracellularly. The consequences of these three mechanisms on the chemolithoautotrophic community have however not been studied. The first sulfur oxidizing mechanism has been shown to affect the chemolithoautotrophic

community in sediments only under laboratory conditions (15) while the third mechanisms may directly involve chemolithoautotrophic Beggiatoaceae as some species are known to grow autotrophically (16). Accordingly, we hypothesize that the presence of these sulfur oxidation regimes as well as the depletion of O_2 and NO_3^- will result in a strong seasonality in both the chemolithoautotrophic activity and community structure under natural conditions.

To examine the above hypothesis, we conducted a multidisciplinary study with intact sediments of Lake Grevelingen, involving both geochemistry and microbiology. Field sampling was conducted during spring (oxygenated bottom waters) and summer (oxygen depleted bottom waters). The dominant sulfur oxidation mechanism was geochemically characterized by sediment microsensor profiling (O_2, H_2S, pH) whereas the abundance of cable bacteria and Beggiatoaceae was performed with fluorescence *in situ* hybridization (FISH). General bacterial diversity was assessed by 16S rRNA gene amplicon sequencing and the analysis of phospholipid derived fatty acids (PLFA). PLFA analysis combined with ^{13}C stable isotope probing (PLFA-SIP) provided the activity and community composition of chemolithoautotrophs in the sediment. This approach was complemented by the analysis of genes involved in dark CO_2 fixation, *i.e.,* characterizing diversity and the abundance of the genes *cbbL* and *aclB* that code for key enzymes in Calvin-Benson Bassham (CBB) and reductive tricarboxylic acid (rTCA) carbon fixation pathways. This multidisciplinary research showed strong temporal and spatial shifts of the chemolithoautotrophic composition and activity in relation to the seasonal hypoxia and the main sulfur oxidation mechanisms present in the sediments of the marine Lake Grevelingen.

MATERIAL AND METHODS

Study site and sediment sampling

Lake Grevelingen is a former estuary located within the Rhine-Meuse-Scheldt delta area of the Netherlands, which became a closed saline reservoir (salinity ~30) by dam construction at both the land side and sea side in the early 1970s. Due to an absence of tides and strong currents, Lake Grevelingen experiences a seasonal stratification of the water column, which in turn, leads to a gradual depletion of the oxygen in the bottom waters (17). Bottom water oxygen at the deepest stations typically starts to decline in April, reaches hypoxic conditions by end of May (O_2 < 63 µM), further decreasing to anoxia in August (O_2 <0.1 µM), while the re-oxygenation of the bottom water takes place in September (14).

To study the effects of the bottom water oxygenation on the benthic chemolithoautotrophic community we performed a field sampling campaign on March 13th, 2012 (before the start of the annual O_2 depletion) and August 20th, 2012 (at the height of the annual O_2 depletion). Detailed water column, pore water and solid sediment chemistry of Lake Grevelingen over the year 2012 have been previously reported (14; 17, 18). Sediments were recovered at three stations along a depth gradient within the Den Osse basin, one of the

deeper basins in Marine Lake Grevelingen: Station 1 (S1) was located in the deepest point (34 m) of the basin (51.747°N, 3.890°E), Station 2 (S2) at 23 m depth (51.749°N, 3.897°E) and Station 3 (S3) at 17 m depth (51.747°N, 3.898°E). Intact sediment cores were retrieved with a single core gravity corer (UWITEC) using PVC core liners (6 cm inner diameter, 60 cm length). All cores were inspected upon retrieval and only cores with a visually undisturbed surface were used for further analysis.

Thirteen sediment cores for microbial analysis were collected per station and per time point: two cores for phospholipid-derived fatty acid analysis combined with stable isotope probing (PLFA-SIP), two cores for nucleic acid analysis, four cores for ^{13}C-bicarbonate labeling, three cores for microelectrode profiling, one core for quantification of cable bacteria (see supplement), and one core for quantification of Beggiatoaceae (see supplement). Sediment cores for PLFA extractions were sliced manually on board the ship (5 sediment layers; sectioning at 0.5, 1, 2, 4, and 6 cm depth). Sediment slices were collected in Petri dishes, and replicate depths were pooled and thoroughly mixed. Homogenized sediments were immediately transferred to centrifuge tubes (50 ml) and placed in dry ice until further analysis. Surface sediments in August consisted of a highly porous "fluffy" layer that was first left to settle after core retrieval. Afterwards, the top 1 cm thick layer was recovered through suction (rather than slicing). Sediment for nucleic acid analysis was collected by slicing manually at a resolution of 1 cm up to 5 cm depth. Sediment samples were frozen in dry ice, transported to the laboratory within a few hour and placed at −80°C until further analysis.

Microsensor profiling

Oxygen depth profiles were recorded with commercial microelectrodes (Unisense, Denmark; tip size: 50 µm) at 25−50 µm resolution. For H_2S and pH (tip size: 50 and 200 µm), depth profiles were recorded at 200 µm resolution in the oxic zone, and at 400 or 600 µm depth resolution below. Calibrations for O_2, pH and H_2S were performed as previously described (14; 19). ΣH_2S was calculated from H_2S based on pH measured at the same depth using the R package AquaEnv (20). The oxygen penetration depth (OPD) is operationally defined as the depth below which $[O_2] < 1$ µM, while the sulfide appearance depth (SAD) is operationally defined as the depth below which $[H_2S] > 1$ µM. The diffusive oxygen uptake (DOU) was calculated from the oxygen depth profiles as previously described in detail (15).

DNA extraction and 16S rRNA gene amplicon sequencing

DNA from 0 cm to 5 cm sediment depth (in 1 cm resolution) was extracted using the DNA PowerSoil® Total Isolation Kit (Mo Bio Laboratories, Inc., Carlsbad, CA). Nucleic acid concentrations were quantified spectrophotometrically (Nanodrop, Thermo Scientific, Wilmington, DE) and checked by agarose gel electrophoresis for integrity. DNA extracts were kept frozen at –80°C.

Sequencing of 16S rRNA gene amplicons was performed on the first cm of the sediment (0–1 cm depth) in all stations in March and August as described before (21). Further details are provided in the SI. The 16S rRNA gene amplicon reads (raw data) have been deposited in the NCBI Sequence Read Archive (SRA) under BioProject number PRJNA293286. The phylogenetic affiliation of the 16S rRNA gene sequences was compared to release 119 of the SILVA NR SSU Ref database (http://www. arb-silva.de/; 22) using the ARB

software package (23). Sequences were added to a reference tree generated from the Silva database using the ARB Parsimony tool.

Sediment incubations and PLFA-SIP analysis

Sediment cores were labeled with ^{13}C-bicarbonate to determine the chemolithoautotrophic activity and associated bacterial community by tracing the incorporation of ^{13}C into bacterial PLFA. To this end, four intact cores were sub-cored with smaller core liners (4.5 cm inner diameter; 20 cm height). *In situ* bottom water was kept over the sediment and no gas headspace was present. Cores were kept inside a closed cooling box during transport to the laboratory.

Stock solutions of 80 mM of ^{13}C-bicarbonate (99% ^{13}C; Cambridge Isotope Laboratories, Andover, Ma, USA) were prepared as previously described (11). ^{13}C-bicarbonate was added to the sediment from 3 cm above the surface to 8 cm deep in the sediment cores in aliquots of 100 µl through vertically aligned side ports (0.5 cm apart) with the line injection method (24). March sediments were incubated at 17±1°C in the dark for 24 h and continuously aerated with ^{13}C-saturated air to maintain 100% saturated O_2 conditions as those found *in situ*, but avoiding the stripping of labeled CO_2 from the overlying water (15). In August, sediments were incubated at 17±1°C in the dark for 40 h to ensure sufficient labeling as a lower activity was expected under low oxygen concentrations. In August, oxygen concentrations in the overlying water were maintained near *in situ* O_2 levels measured in the bottom water (S1: 0−4% saturation, S2: 20−26%, S3: 35−80%). A detailed description of aeriation procedures can be found in the SI.

At the end of the incubation period, sediment cores were sliced in five depth intervals (as described for PLFA sediment cores sliced on board) thus obtaining two replicate slices per sediment depth and per station. Sediment layers were collected in centrifuge tubes (50 ml) and wet volume and weight were noted. Pore water was obtained by centrifugation (4500 rpm for 5 min) for dissolved inorganic carbon (DIC) analysis, and sediments were lyophilized for PLFA analysis. Biomarker extractions were performed on freeze dried sediment as described before (25) and ^{13}C-incorporation into PLFA was analyzed as previously reported (11). Nomenclature of PLFA can be found in the SI. Detailed description of the PLFA calculations can be found in the literature (15; 26). Total dark CO_2 fixation rates (mmol C m^{-2} d^{-1}) are the depth-integrated rates obtained from the 0−6 cm sediment interval.

Quantitative PCR

To determine the abundance of chemolithoautotrophs we quantified the genes coding for two enzymes involved in dark CO_2 fixation pathways: the large subunit of the RubisCO enzyme (ribulose 1,5-bisphosphate carboxylase/oxygenase) *cbb*L gene, and the ATP citrate lyase *aclB* gene. Abundance of the RubisCO *cbb*L gene was estimated by using primers K2f/V2r, specific for the forms IA and IC of the RuBisCO form I large subunit gene *cbbL* which is present in obligately and facultatively lithotrophic bacteria (27, 28). The abundance of ATP citrate lyase *aclB* gene was quantified by using the primer set aclB_F/aclB_R, which is based on the primers 892F/1204R (29), specific for the ATP citrate lyase β gene of chemoautotrophic bacteria using the rTCA pathway, with several nucleotide differences introduced after

aligning n = 100 sequences of *aclB* gene fragments affiliated to Epsilonproteobacteria (See Table S1 for details).

The quantification of *cbb*L and *aclB* genes via quantitative PCR (qPCR) was performed in 1 cm resolution for the sediment interval between 0–5 cm depth in all stations in both March and August. qPCR analyses were performed on a Biorad CFX96^{TM} Real-Time System/C1000 Thermal cycler equipped with CFX Manager^{TM} Software. All qPCR reactions were performed in triplicate with standard curves from 10^0 to 10^7 molecules per microliter. Standard curves and qPCR reactions were performed as previously described (30). Melting temperatures (Tm) are listed in Table S1, qPCR efficiencies (*E*) for *aclB* gene and *cbbL* gene amplifications were 70 and 82%, respectively. Correlation coefficients for standard curves were ≥ 0.994 for *aclB* gene and ≥0.988 for *cbbL* gene amplification.

PCR amplification and cloning

Amplifications of the RubisCO *cbb*L gene and the ATP citrate lyase *aclB* gene were performed with the primer pairs specified in Table S1. The PCR reaction mixture was the following (final concentration): Q-solution (PCR additive, Qiagen, Valencia, CA) 1×; PCR buffer 1×; BSA (200 µg ml^{-1}); dNTPs (20 µM); primers (0.2 pmol µl^{-1}); $MgCl_2$ (1.5 mM); 1.25 U Taq polymerase (Qiagen, Valencia, CA). PCR conditions for these amplifications were the following: 95°C, 5 min; 35 × [95°C, 1 min; Tm, 1 min; 72°C, 1 min]; final extension 72°C, 5 min. PCR products were gel purified (QIAquick gel purification kit, Qiagen, Valencia, CA) and cloned in the TOPO-TA cloning® kit (Life Technologies, Carlsbad, CA) and transformed in *E. coli* TOP10 cells following the manufacturer's recommendations. Recombinant plasmid DNA was sequenced using M13R primer by BASECLEAR (Leiden, The Netherlands).

Sequences were aligned with MEGA5 software (31) by using the alignment method ClustalW. The phylogenetic trees of the *cbb*L and *aclB* genes were computed with the Neighbour-Joining method (32). The evolutionary distances were estimated using the Jukes-Cantor method (33) for DNA sequences and with the Poisson correction method for protein sequences (34) with a bootstrap test of 1,000 replicates. Sequences were deposited in NCBI with the following accession numbers: KT328918–KT328956 for *cbb*L gene sequences and KT328957–KT329097 for *aclB* gene sequences.

Further details on experimental procedures and methods are found in the Supplementary Information.

RESULTS

Geochemical characterization

The seasonal variation of the bottom water oxygen concentration in Lake Grevelingen strongly influenced the porewater concentrations of O_2 and H_2S. In March, bottom waters were fully oxygenated at all stations (299–307 µmol L^{-1}), oxygen penetrated 1.8–2.6 mm deep in the sediment, and no free sulfide was recorded in the first few centimeters (Table 1). The width of the suboxic zone, operationally defined as the sediment layer located between the oxygen penetration depth (OPD) and the sulfide appearance depth (SAD), varied between 16–39 mm across the three stations in March 2012. In contrast, in August, oxygen

was strongly depleted in the bottom waters at S1 (<0.1 μmol L^{-1}) and S2 (11 μmol L^{-1}), and no O_2 could be confidently detected by microsensor profiling in the surface sediment at these two stations. At station S3, the bottom water O_2 remained higher (88 μmol L^{-1}), and oxygen penetrated down to 1.1 mm. In August, free sulfide was present near the sediment-water interface at all three stations, and the accumulation of sulfide in the pore water increased with water depth (Fig. 1a). Depth pH profiles showed much larger variation between stations in March compared to August (Fig. 1a). The pH profiles in S1 and S3 in March were similarly characterized by highest values in the oxic zone and low pH values (pH < 6.5) in the suboxic zone. The pH depth profile in S2 showed an inverse pH profile with a pH minimum in the oxic layer and a subsurface maximum below. The pH profiles at S1 and S3 in August 2012 showed a gradual decline of pH with depth, while the pH profile at S2 in August was more or less constant with depth.

Bacterial diversity by 16S rRNA gene amplicon sequencing

The general diversity of bacteria was assessed by 16S rRNA gene amplicon sequencing analysis, which was applied to the surface sediments (0−1 cm) of all stations in both March and August. Approximately 50% of the reads were assigned to three main clades: Gamma-, Delta-, and Epsilonproteobacteria (Fig. 2). The remaining reads were distributed amongst the orders Bacteroidetes (14%), Planctomycetes (6%), Alphaproteobacteria (3%), other orders (20%), the candidate phylum WS3 (2%) and unassigned (5%) (given as the average of the three stations and both seasons).

Reads classified within the Gammaproteobacteria were more abundant in March during oxygenated bottom water conditions than in August (Fig. 2). The majority of these reads were assigned to the orders Alteromonadales, Chromatiales and Thiotrichales. The first order includes chemoheterotrophic bacteria that are either strict aerobes or facultative anaerobes (35). Phylogenetic comparison revealed that the reads assigned to the Chromatiales group were closely related to the Granulosicoccaceae, Ectothiorhodospiraceae, and Chromatiaceae families (Fig. S1). Reads falling in the Thiotrichales group were closely related to sulfur-oxidizing bacteria from the Thiotrichaceae family with 30% of the sequences related to the genera '*Candidatus* Isobeggiatoa', '*Ca*. Parabeggiatoa' and *Thiomargarita* (Fig. S2). It has been recently proposed that the genera *Beggiatoa*, *Thiomargarita* and *Thioploca* should be reclassified into the originally published monophyletic family of Beggiatoaceae (36, 37), and so here, these genera will be further referred to as Beggiatoaceae. Most of the reads assigned to the Beggiatoaceae came from station S2 in spring, whereas the percentage of reads assigned to sulfur oxidizers from the order Thiotrichales decreased in August when oxygen concentrations in the bottom water were low.

Within the Deltaproteobacteria, reads were assigned to the orders Desulfarculales and Desulfobacterales (Fig. S3). Reads within the order of Desulfobacterales were mainly assigned to the families Desulfobacteraceae (between 10−20%) and Desulfobulbaceae (~5%) (Fig. 2). Additional phylogenetic comparison revealed that within the Desulfobulbaceae, 60% of reads, obtained from the three stations in both seasons, clustered within the genus *Desulfobulbus*, of which 30% were related to the electrogenic sulfur-oxidizing cable bacteria (Fig. S4). Overall, the relative abundance of reads assigned to the

Desulfobulbaceae family was similar between the two seasons in S2 and S3, whereas in S1 the percentage of reads was approximately 4.5-fold higher in March compared to August (Fig. 2). In contrast, the relative abundance of reads assigned to the Desulfarculales and Desulfobacteraceae increased in August during hypoxia (Fig. 2), and phylogenetic comparison revealed typical sulfate reducer genera *Desulfococcus*, *Desulfosarcina*, and *Desulfobacterium*, indicative of anaerobic metabolism (Fig. S5a–c).

All Epsilonproteobacteria reads were assigned to the order Campylobacterales, such as the Campylobacteraceae and Helicobacteraceae families. Phylogenetic comparison showed that the reads were closely related to the genera *Sulfurovum*, *Sulfurimonas*, *Sulfurospirillum*, *Arcobacter* (Fig. S6a–d), all capable of sulfur oxidation with oxygen or nitrate (38). The percentage of reads assigned to the Epsilonproteobacteria in August was lower than those in March, with highest numbers present in S2 in March (~6%), (Fig. 2).

Bacterial community structure by phospholipid derived fatty acid analysis

The relative concentrations of phospholipid derived fatty acid (PLFA) were determined to a depth of 6 cm and were analyzed by principal component analysis (PCA) to determine differences in bacterial community structure (Fig. 3). A total of 22 individual PLFA, each contributing more than 0.1% to the total PLFA biomass, were included in this analysis. Samples with low total PLFA biomass (less than one standard deviation below the mean of all samples) were excluded. The PCA analysis indicated that 73% of the variation within the dataset was explained by the first two principal components (PC). While PC1 correlated with sediment depth (particularly for the March samples), PC2 clearly exposed differences in the bacterial community structure between seasons (Fig. 3a). Surface sediments (0–1 cm) were characterized by high relative concentrations of C16 and C18 monounsaturated PLFA. In contrast, ai15:0, i17:1ω7c, and 10Me16:0 were more abundant in deeper sediments (Fig. S7a). The surface sediment showed an increased contribution of iso, anteiso and branched PLFAs in August relative to March, and this was more similar to the deeper sediments from March (Fig. 3a). Nonetheless, August sediments also showed a higher abundance of 16:0, 14:0, and 18:1ω9c compared to the deeper sediment layers in March (Fig. S7a).

Chemolithoautotrophic activity and community by ^{13}C-phospholipid fatty acids analysis

Incorporation of ^{13}C-labeled dissolved inorganic carbon was found in bacterial PLFAs after 24 to 40 hours of incubation (Fig. S7b). Depth integrated dark CO_2 fixation rates based on ^{13}C-incorporation (Table 1) showed a significant difference between seasons and stations ($p=0.0005$). In March, chemolithoautotrophy increased with water depth, while in August, the opposite trend was observed. The dark CO_2 fixation rate in March for S1 was the highest across all seasons and stations, but dropped by one order of magnitude in August. In contrast, at the intermediate station (S2), the dark CO_2 fixation rate was only two times higher in March compared to August, while in the shallowest station (S3) the depth integrated rates were not significantly different between seasons ($p=0.56$).

The depth distribution of the chemolithoautotrophic activity also differed between seasons ($p=0.02$; Fig. 1b). In August, the chemolithoautotrophic activity was restricted to the upper cm of the sediment at all

stations while in March, chemolithoautotrophic activity was measured deep into the sediment (up to 4 cm). In stations S1 and S3 during March, the activity depth profile showed high activities down to 4 cm, whereas at S2 chemolithoautotrophy only extended down to 2 cm with highest activity in the top 1 cm. This distinction between the depth distributions of chemolithoautotrophy at S2 versus S1/S3 in March correlated with the distinct pH profiles observed for S2 versus S1/S3 (Fig. 1c).

The PLFA ^{13}C-fingerprints were analyzed by PCA to identify differences in chemolithoautotrophic community. Only PLFA that contributed more than 0.1% to the total ^{13}C-incorporation and sediment layers that showed chemolithoautotrophy rates higher than 0.01 μmol C cm^{-3} d^{-1} were taken into account in this analysis. Because chemolithoautotrophy rates were low in August, the PCA analysis mainly analyzed the chemolithoautotrophic communities in March (Fig. 3b). Within the dataset, 64% of the variation was explained by two principal components. PC1 revealed a clear differentiation between station S2, and stations S1 and S3 (Fig. 3b) in agreement with the distinct pH profiles described for March (Fig. 1a). S2 sediment horizons showed a higher contribution of monounsaturated C16 and C18 fatty acids, whereas sediments from S1 and S3 revealed an increased ^{13}C-incorporation into fatty acids with iso and anteiso C15 and saturated C14 PLFA (Fig. S7c), together these results indicate distinct chemolithoautotrophic microbial assemblages between S2 and S1/S3. On the contrary, the three sediment samples from August (that had sufficient ^{13}C-incorporation for the analysis) did not cluster in the PCA analysis and exhibited divergent PLFA profiles, thus the chemolithoautotrophic bacterial community for August could not be characterized further based on PLFA analysis.

Chemolithoautotrophic carbon fixation pathways

Various CO_2 fixation pathways are used by autotrophic bacteria (for detailed reviews see 39, 40). The CBB pathway is utilized by cyanobacteria and many aerobic or facultative aerobic proteobacteria of the alpha, beta and gamma subgroups whereas the rTCA pathway operates in anaerobic or microaerobic members of phyla such as Chlorobi, Aquificae, proteobacteria of the delta and epsilon subgroups and Nitrospirae (39). The spatial and temporal distribution of bacteria possessing these two autotrophic carbon fixation pathways was studied by quantifying the abundance of *cbbL* gene (CBB pathway) (28) and *aclB* gene (rTCA pathway) (38, modified in this study) by quantitative PCR down to 5 cm sediment depth (Fig. 4).The diversity of *cbbL* and *aclB* gene sequences obtained from the surface sediments (0–1cm) was analyzed (Fig. 5).

Significant differences were found in the abundance of *cbbL* and *aclB* genes ($p = 5.7 \times 10^{-7}$) and between season (p=0.002), but not between stations (Fig. 4). The abundance of the *cbbL* gene copies was at least 2-fold higher than that of the *aclB* gene in March and August in all stations ($p = 5\times10^{-5}$). In March, the depth profiles of *cbbL* gene showed a similar trend in stations S1 and S3 with a decreasing gene abundance from the surface towards deeper layers, but depth integrated abundance of the *cbbL* gene was more than two-fold higher in S1 than in S3 (Fig. 4a). The depth distribution of the *cbbL* gene in the deepest station (S1) differed between seasons (p=0.004), with lower gene copy abundances in the top 4 cm in August (Fig. 4a).

In contrast, in the shallow station (S3), which experiences less seasonal fluctuations in bottom water O_2, the *cbbL* gene copy number did not differ significantly between seasons (p=0.4), except for a sharp decrease in the top cm of the sediment. In station S2, abundance and depth distribution of *cbbL* gene copies was similar between the two seasons (p=0.3). All detected *cbbL* gene sequences clustered with uncultured Gammaproteobacteria clones, assigned to the orders Chromatiales and Thiotrichales (both *cbbL*1 and *cbbL*2 clusters) reported in intertidal sediment from Lowes Cove, Maine (28).

The abundance of the *aclB* gene significantly differed between months (p=0.0004) and stations (p=0.04). Similar depth profiles of the *aclB* gene were detected in stations S1 and S3, with subsurface maxima in deeper sediments (at 3–4 cm and 2–3 cm deep for S1 and S3 respectively, Fig. 4b). Station S2 showed the highest *aclB* gene abundance in March, which remained constant with sediment depth (p=0.86). In August, *aclB* gene abundance decreased substantially in S2 (p<0.001). All stations showed a uniform distribution of the *aclB* gene abundance with depth in August. Bacterial *aclB* gene sequences in surface sediments (0−1 cm) of all stations were predominantly related to *aclB* sequences of Epsilonproteobacteria (Fig. 5b). Within the Epsilonproteobacteria, sequences clustered in six different subclusters and were mainly affiliated to bacteria in the order of Campylobacterales, *i.e.,* to the genera *Sulfuricurvum, Sulfurimonas, Thiovulum, Arcobacter,* and macrofaunal endosymbionts. As observed for the *cbbL* gene, no clustering of sequences was observed according to station or season (Fig. 5b).

Quantification of cable bacteria and filamentous Beggiatoaceae

We performed a detailed microscopy-based quantification of the biovolume of sulfur oxidizing cable bacteria and filamentous Beggiatoaceae because both groups have been reported to govern the sediment geochemistry and sulfur cycling in sediments of Lake Grevelingen (14), and thus are likely to influence the chemolithoautotrophic community. Biovolume data of both filamentous bacteria for S1 have been reported before (14) whereas data for S2 and S3 are novel results from the 2012 campaign. In March, high biovolumes of cable bacteria were detected in S1 and S3 (Table 1) with filaments present throughout the suboxic zone until a maximum depth of 4 cm (Fig. 1c). At the same time, cable bacteria were absent in S2 (Fig. 1c). In August, cable bacteria were only detected between 1 and 2 cm deep at the deepest station (S1), albeit at abundances that were close to the detection limit of the technique. Beggiatoaceae were found in all three stations in March, although the biovolume at S2 was one order of magnitude higher than in the other two stations (Table 1). In station S2, Beggiatoaceae were uniformly distributed up to the sulfide appearance depth (Fig. 1c). In August, Beggiatoaceae were no longer detectable in stations S1 and S3 (Table 1), while at S2, filaments were no longer found in deeper sediment, but formed a thick mat at the sediment-water interface (Fig. 1c).

DISCUSSION

Temporal shifts of chemolithoautotrophy and the associated bacterial assemblages

Together, our geochemical and microbiological characterization of the sediments of Lake Grevelingen indicates that the availability of electron acceptors (O_2, NO_3^-) constitutes the main environmental factor controlling the activity of the chemolithoautotrophic bacterial community. In the deeper basins of Lake Grevelingen (below water depth of 15 m), the electron acceptor availability changes on a seasonal basis due to the establishment of summer hypoxia (14; 18). In March, when high oxygen levels are found in the bottom waters, the chemolithoautotrophy rates were substantially higher than in August when oxygen in the bottom water was depleted to low levels (Fig. 1b; Table 1). Moreover in August, the chemolithoautotrophy rates showed a clear decrease with water depth (from S3 to S1) in line with the decrease of the bottom water oxygen concentration over depth.

The 16S rRNA gene amplicon sequencing analysis in our study reveals that the response of the chemolithoautotrophic bacterial community in the surface sediments of Lake Grevelingen is associated with the seasonal changes in bottom water oxygen (Fig. 2). Generally, Lake Grevelingen surface sediments harbor a distinct microbial community compared to other surface sediments such as coastal marine (North Sea), estuarine and Black Sea sediments (8, 9; 12) studied by 16S rRNA gene amplicon sequencing analysis.

In March, with oxic bottom waters, the microbial community in the top centimeter of the sediment at all three stations was characterized by high abundances of Epsilon- and Gammaproteobacteria, which are known chemolithoautotrophic sulfur-oxidizers (e.g. capable of oxidizing sulfide, thiosulfate, elemental sulfur and polythionates) using oxygen or nitrate as electron acceptor (38; 41−43). In August, the lack of electron acceptors (O_2, NO_3^-) in the bottom water was accompanied by a decrease in the relative abundance of these Gammaproteobacteria and Epsilonproteobacteria. At the same time, the numbers of reads related to the Desulfobacteraceae family increased in the top centimeter of the sediment, and a shift in the microbial community structure towards sulfate reducing bacteria related to the genera *Desulfococcus* and *Desulfosarcina* was evident. In coastal sediments, these genera are characteristic in deeper sediment layers experiencing anaerobic mineralization (44−46), and thus, they are not unexpected in surface sediments during strongly hypoxic (S2) and anoxic (S1) conditions encountered in August. Shifts in PLFA patterns are in agreement with the temporal difference in the bacterial community (Fig. 3a), with more PLFAs found in Gammaproteobacteria and Epsilonproteobacteria in March (*i.e.*, 16:1ω7c and 18:1 ω7c; 47) as opposed to more PLFAs found in sulfate reducing bacteria in the Deltaproteobacteria in August (*i.e.*, ai15:0, i17:1ω7c, 10Me16:0; 26; 48, 49). However, sediments below the OPD in March have PLFA patterns that are more similar to those of surface sediments in August, in agreement with the observation that anaerobic metabolism such as sulfate reduction prevail in deeper anoxic sediments also in March.

Spring: Activity and diversity of chemolithoautotrophic bacteria

Although the availability of soluble electron acceptors (O_2, NO_3^-) in the bottom water is important, our data show that it cannot be the only structuring factor of the chemolithoautotrophic communities. In March 2012, all the three stations examined experienced similar bottom water O_2 and NO_3^- concentrations (Table 1), but still substantial differences were observed in the composition of the chemolithoautotrophic communities as determined by PLFA-SIP (Fig. 3b), as well as in the depth distribution of the chemolithoautotrophy rates in the sediment (Fig. 1b). We attribute these differences to the presence of specific sulfur oxidation mechanisms that are active in the sediments of Lake Grevelingen (14). In March 2012, based on FISH counts and microsensor profiles two separate sulfur oxidation regimes were active at the sites investigated: sites S1 and S3 were impacted by electrogenic sulfur oxidation by cable bacteria, while site S2 was dominated by sulfur oxidation via nitrate-storing, filamentous Beggiatoaceae. Each of these two regimes is characterized by a specific sulfur-oxidizing microbial community and a particular depth distribution of the chemolithoautotrophy. We now discuss these two regimes separately in more detail.

Electrogenic sulfur oxidation

In March, stations S1 and S3 (Fig. 1a) showed the geochemical fingerprint of electrogenic sulfur oxidation (e-SOx) consisting of a centimeter-wide suboxic zone that is characterized by acidic pore waters (pH < 7) (50, 51). Electrogenic sulfur oxidation is attributed to the metabolic activity of cable bacteria (52), which are long filamentous bacteria related to the sulfate reducing genus *Desulfobulbus* that extend centimeters deep into the sediment (53). The observed depth-distribution of cable bacteria at S1 and S3 (Fig. 1c) was congruent with the geochemical fingerprint of e-SOx. Cable bacteria couple the oxidation of sulfide in deeper layers to the reduction of oxygen near the sediment-water interface, by channeling electron along their longitudinal axis (long-distance electron transport). Note that stations S1 and S3 also contained some Beggiatoaceae. However, they attained low biovolumes and were only found at certain depths, suggesting that they did not play a significant role in sulfur oxidation.

When e-SOx was present in the sediment (sites S1 and S3 in March), the chemolithoautotrophic activity penetrated deeply into the sediment and was evenly distributed throughout the suboxic zone (Fig. 1b). These field observations confirm previous laboratory incubations in which cable bacteria were induced under oxic conditions in homogenized sediments, and a highly similar depth pattern of deep chemolithoautotrophy was noted (15). This deep dark CO_2 fixation is unexpected in two ways. Firstly, cable bacteria are likely not responsible for the deep CO_2 fixation although they do perform sulfur oxidation, as cable bacteria from Lake Grevelingen have been shown to incorporate organic carbon rather than inorganic carbon (15). Secondly, chemolithoautotrophy is generally dependent on reoxidation reactions, but there is no transport of oxygen or nitrate to centimeters depth in these cohesive sediments, and so the question is: how can chemolithoautotrophic reoxidation occur in the absence of suitable electron acceptors?

To reconcile these observations, it was proposed that in incubated electro-active sediments from Lake Grevelingen, heterotrophic cable bacteria can form a sulfur-oxidizing consortium with chemolithoautotrophic Gamma- and Epsilonproteobacteria throughout the suboxic zone (15). The results

obtained in our study provide various lines of evidence that support the existence of such a consortium in intact sediment cores. The PLFA-SIP patterns in S1 and S3 (Fig. 3b) showed major ^{13}C-incorporation in PLFA which are present in sulfur-oxidizing Gamma- and Epsilonproteobacteria (42; 54, 55, 56), and this occurred throughout the top 5 cm of the sediment corresponding to the zone of e-SOx activity. In addition, the depth profiles of genes involved in dark CO_2 fixation (Fig. 4) revealed chemolithoautotrophic Gammaproteobacteria using the CBB cycle as well as Epsilonproteobacteria using the rTCA cycle, which confirms the potential dark CO_2 fixation by both bacterial groups deep in the sediment. The higher abundance of *cbbL* genes in S1 compared to S3 indicates a greater chemolithoautotrophic potential of Gammaproteobacteria, which may explain the two-fold higher total chemolithoautotrophy rate encountered in S1. Moreover, the peak in *aclB* gene abundance found in deeper sediment suggests that Epsilonproteobacteria could play an important role in sulfur oxidation in the deeper suboxic zone in both stations. Clearly, a consortium could sustain the high rates of chemolithoautotrophy throughout the suboxic zone. It has been speculated that chemolithoautotrophs use the cable bacteria as an electron sink in the absence of an electron acceptor like O_2 or NO_3^- in centimeter deep sediments (15). However the question still remains as to how the Gamma- and Epsilonproteobacteria are metabolically linked to the cable bacteria (Fig. 6).

In March, stations S1 and S3 also showed a higher contribution of fatty acids occurring in the sulfate reducing Deltaproteobacteria (11; 48; 57) compared to the PLFA-SIP profiles in station S2 (Fig. 3b). Deltaproteobacteria such as *Desulfobacterium autotrophicum* and *Desulfocapsa* sp., as identified by 16S rRNA gene sequencing, are known to grow as chemolithoautotrophs by performing H_2 oxidation or S^0-disproportionation (58, 59; Fig. 6), and are important contributors to the chemolithoautotrophic activity in coastal sediments (11; 60). However, a further identification of the chemolithoautotrophic Deltaproteobacteria through the functional genes related to carbon fixation pathways was not performed in this study. Although it is known that autotrophic Deltaproteobacteria mainly use the reverse TCA cycle or the reductive acetyl-CoA pathway (40), further development of the functional gene approach, by designing specific primers is necessary to determine and clarify the diversity of Deltaproteobacteria involved in the chemolithoautotrophic activity.

Overall, we hypothesize that such a diverse assemblage of chemolithoautotrophic bacteria in the presence of cable bacteria is indicative of a complex niche partitioning between these sulfur-oxidizers (Gamma-, Epsilon-, and Deltaproteobacteria). In sulfidic marine sediments found in tidal and deep sea habitats, complex S^0 niche partitioning have been proposed where uncultured sulfur-oxidizing Gammaproteobacteria mainly thrive on free sulfide, the epsilonproteobacterial Sulfurimonas/Sulfurovum group oxidizes elemental sulfur, and members of the deltaproteobacterial Desulfobulbaceae family may perform S^0-disproportionation (61).

Nitrate-storing filamentous Beggiatoaceae

Nitrate-storing filamentous Beggiatoaceae glide through the sediment transporting their electron acceptor (intracellular vacuoles filled with high concentrations of NO_3^-) into deeper sediment and electron donor (intracellular granules of elemental sulfur) up to the surface, and in doing so, they oxidize free sulfide to sulfate in a two-step process that creates a wide suboxic zone (14; 62, 63; Fig. 6). In March, the microsensor depth profiles at S2 (Fig. 1a) revealed a cm-thick suboxic zone with a subsurface pH minimum at the OPD followed by a pH maximum at SAD, which is the characteristic geochemical fingerprint of sulfur oxidation by nitrate-storing Beggiatoaceae (14; 63). At the same time, microscopy revealed high biovolumes of Beggiatoaceae that were uniformly distributed throughout the suboxic zone (Fig. 1c), and more than half the filaments found were thicker than 15 µm indicating potential nitrate storage. Together these results corroborate the indications of the dominant sulfur-oxidation mechanism suggested by the geochemical fingerprint.

The chemolithoautotrophy depth profile at S2 in March (Fig. 1b) recorded higher activities in the top 1 cm and chemolithoautotrophic activity penetrated down only to 2 cm (at the sulfide appearance depth). The similar depth distribution of Beggiatoaceae and chemolithoautotrophic activity suggests that dark CO_2 fixation was primarily carried out by the nitrate-storing Beggiatoaceae. Beggiatoaceae can indeed grow as obligate or facultative chemolithoautotrophs depending on the strain (64). The PLFA-SIP analysis further supported chemolithoautotrophy by Beggiatoaceae as the PLFA patterns obtained at S2 resembled those of *Beggiatoa* mats encountered in sediments associated with gas hydrates (56).

However, the CO_2 fixation by Beggiatoaceae could be complemented by the activity of other chemolithoautotrophs. Beggiatoaceae have previously been reported to co-occur with chemolithoautotrophic nitrate-reducing and sulfur-oxidizing Epsilonproteobacteria (*Sulfurovum* and *Sulfurimonas*) in the deep sea Guyamas basin (65). Interestingly, station S2 in March showed the highest abundance of *aclB* gene copies of all stations and seasons (Fig. 4b), and in addition, had the highest relative percentage of 16S rRNA gene read sequences assigned to the Epsilonproteobacteria (Fig. 2). Therefore, the dark CO_2 fixation at station S2 is likely caused by both the motile, vacuolated Beggiatoaceae as well as the sulfur-oxidizing Epsilonproteobacteria. Yet, as was the case of the cable bacteria above, the metabolic link between Beggiatoaceae and the Epsilonproteobacteria remains currently unknown. However, it seems possible that internally stored NO_3^- is released into the sediment once *Beggiatoa* filaments lyse, allowing sulfur-oxidation with NO_3^- by Epsilonproteobacteria.

Summer: Activity and diversity of chemolithoautotrophic bacteria

In August, when the O_2 levels in the bottom water decreased substantially, a third geochemical regime was observed at all stations, which was different from the regimes associated with cable bacteria or nitrate-storing Beggiatoaceae. The microsensor profiling revealed an upward diffusive transport of free sulfide to the top millimeters of the sediment, which was produced in deeper sediment horizons through sulfate reduction (Fig. 1a). The uniform decrease in pH with depth is consistent with sediments dominated by sulfate reduction (51). As noted above, the chemolithoautotrophy rates strongly decreased compared to

March and were restricted to the very top of the sediment. Chemolithoautotrophic activity showed a close relation with the bottom water oxygen concentration. The number of gene copies of the two carbon fixation pathways investigated (CBB and rTCA) also decreased under hypoxic conditions (Fig. 4), suggesting a strong dependence of subsurface chemolithoautotrophy on the availability of oxygen in bottom waters.

The highest chemolithoautotrophy rate was recorded at the shallower station (S3), which was the only station in August where O_2 was found to diffusive into the sediment (Table 1), thus supporting aerobic sulfur oxidation at a shallow oxic-sulfidic interface in the sediment (51). Several studies have shown that chemolithoautotrophy ceases in the absence of oxygen in the overlying water column (15; 45; 60). Such full anoxia occurred in the deepest station (S1), but still limited chemolithoautotrophic activity was recorded in the top layer of the sediment. A possible explanation is that some residual aerobic sulfur oxidizing bacteria were supported by the very low oxygen levels. Alternatively, cable bacteria activity at S1 in spring leads to a buildup of iron (hydr)oxides (FeOOH) in the top of the sediments, which prevents sulfide diffusion to the bottom water during summer anoxia ($3H_2S + 2FeOOH \rightarrow 2FeS + S^0 + 4H_2O$) (14). The elemental sulfur formed in this reaction may support chemolithoautotrophic sulfur disproportionating bacteria (58). At station S2, Beggiatoaceae were found forming a mat at the sediment surface in S2 (Fig. 1b) and chemolithoautotrophy rates were limited to this mat (Fig. 6). Beggiatoaceae can survive hypoxic periods by using stored nitrate as electron acceptor (66), which is thought to be a competitive advantage that leads to their proliferation in autumn in S1 (14). Such survival strategies may be used to produce energy for maintenance rather than growth under hypoxic conditions which would in combination with the low oxygen concentrations explain the low chemolithoautotrophy to biovolume ratio observed in S2 in August compared to March.

CONCLUSION

Coastal sediments harbor a great potential for chemolithoautotrophic activity given the high anaerobic mineralization, which produce a large pool of reduced sulfur in these organic rich sediments. In this study, two environmental factors were identified to regulate the chemolithoautotrophic activity in coastal sediments: seasonal hypoxia and the dominant sulfur oxidation mechanism. In sediments where oxygen, the main electron acceptor for chemolithoautotrophs, is depleted because of seasonal hypoxia, chemolithoautotrophy was strongly inhibited. In addition, it is clear that the different sulfur oxidation mechanism (e.g. canonical sulfur oxidation, electrogenic sulfur oxidation, or sulfur oxidation mediated by vacuolated Beggiatoaceae) observed in the sediment also determine the magnitude and depth distribution of the dark CO_2 fixation, as well as the chemolithoautotrophic bacterial community structure. The seasonal variations in electron acceptors and potentially reduced sulfur species suggest complex niche partitioning in the sediment by the sulfur-oxidizing bacterial community. An in depth study on the availability of different sulfur species in the sediment could shed light on the sulfur preferences by the different bacterial groups. Likewise, the potential mechanism used to metabolically link filamentous sulfur-oxidizers and

chemolithoautotrophic bacteria remains presently unresolved and requires further study. These tight metabolic relationships may ultimately regulate the cycling of sulfur, carbon and even nitrogen in coastal sediments, including (but not limited to) sediments affected by seasonal hypoxia.

ACKNOWLEDGMENTS

We thankfully acknowledge the crew of the R/V Luctor (Peter Coomans and Marcel Kristalijn) and Pieter van Rijswijk for their help in the field during sediment collection, Marcel van der Meer and Sandra Heinzelmann for support onboard and assistance with incubations, Peter van Breugel and Marco Houtekamer for their assistance with stable isotope analysis, Elda Panoto for technical support and Alexandra Vasquez Cardenas for designing Figure 6.

FUNDING INFORMATION

This work was financially supported by several grants from Darwin Centre for Biogeosciences to HTSB (grant no: 3061), LV (grant no: 3062) and FJRM (grant no: 3092), FJRM received funding from the European Research Council under the European Union's Seventh Framework Program (FP7/2007-2013) via ERC grant agreement n° [306933], and RS received support from Danish Council for Independent Research-Natural Sciences.

REFERENCES

1. Soetaert K, Herman PMJ, Middelburg JJ. 1996. A model of early diagenetic processes from the shelf to abyssal depths. Geochim Cosmochim Acta 60:1019–1040.

2. Jørgensen BB, Nelson DC. 2004. Sulfide oxidation in marine sediments: geochemistry meets microbiology. Geol Soc Am 379:61–81.

3. Howarth WR. 1984. The ecological significance of sulfur in the energy dynamics of salt marsh and coastal marine sediments. Biogeochemistry 1:5–27.

4. Brüchert V, Jørgensen BB, Neumann K, Riechmann D, Schlösser M, Schulz H. 2003. Regulation of bacterial sulfate reduction and hydrogen sulfide fluxes in the central Namibian coastal upwelling zone. Geochim Cosmochim Acta 67:4505–4518.

5. Lavik G, Stührmann T, Brüchert V, Van der Plas A, Mohrholz V, Lam P, Mußmann M, Fuchs BM, Amann R, Lass U, Kuypers MMM. 2009. Detoxification of sulphidic African shelf waters by blooming chemolithotrophs. Nature 457:581–584.

6. Sorokin DY, Kuenen JG, Muyzer G. 2011. The microbial sulfur cycle at extremely haloalkaline conditions of soda lakes. Front Microbiol 2:44. doi:10.3389/fmicb.2011.00044.

7. Grote J, Schott T, Bruckner CG, Glöckner FO, Jost G, Teeling H, Labrenz M, Jürgens K. 2012. Genome and physiology of a model Epsilonproteobacterium responsible for sulfide detoxification in marine oxygen depletion zones. Proc Natl Acad Sci U S A 109:506–510.

8. Jessen GL, Lichtschlag A, Struck U, and Boetius A. 2016. Distribution and composition of thiotrophic mats in the hypoxic zone of the Black Sea (150-170 m water depth, Crimea Margin). Front Microbiol 7:1011. doi:10.3389/fmicb.2016.01011.

9. Ye Q, Wu, Y., Zhu, Z., Wang, X., Li, Z., and Zhang, J. 2016. Bacterial Diversity in the surface sediments of the hypoxic zone near the Changjiang Estuary and in the East China Sea. Microbiologyopen 5:323–39. doi:10.1002/mbo3.330.

10. Lenk S, Arnds J, Zerjatke K, Musat N, Amann R, Mußmann M. 2010. Novel groups of Gammaproteobacteria catalyse sulfur oxidation and carbon fixation in a coastal, intertidal sediment. Environ Microbiol 13:758–774.

11. Boschker HTS, Vasquez-Cardenas D, Bolhuis H, Moerdijk-Poortvliet TWC, Moodley L. 2014. Chemoautotrophic carbon fixation rates and active bacterial communities in intertidal marine sediments. PLoS One 9:e101443.

12. Dyksma S, Bischof K, Fuchs BM, Hoffmann K, Meier D, Meyerdierks A, Pjevac P, Probandt D, Richter M, Stepanauskas R, Mußmann M. 2016. Ubiquitous Gammaproteobacteria dominate dark carbon fixation in coastal sediments. The ISME J 10:1939–1953.

13. Diaz RJ, Rosenberg R. 2008. Spreading dead zones and consequences for marine ecosystems. Science 321:926–929.

14. Seitaj D, Schauer R, Sulu-Gambari F, Hidalgo-Martinez S, Malkin SY, Burdorf LDW, Slomp CP, Meysman FJR. 2015. Cable bacteria in the sediments of seasonally-hypoxic basins : a microbial 'firewall' against euxinia. Proc Natl Acad Sci U S A 43:13278–13283.

15. Vasquez-Cardenas D, van de Vossenberg J, Polerecky L, Malkin SY, Schauer R, Hidalgo-Martinez S, Confurius V, Middelburg JJ, Meysman FJ, Boschker HTS. 2015. Microbial carbon metabolism associated with electrogenic sulphur oxidation in coastal sediments. ISME J 9:1966–1978.

16. Nelson DC, Jannasch HW. 1983. Chemoautotrophic growth of a marine *Beggiatoa* in sulfide-gradient cultures. Arch Microbiol 136: 262–269.

17. Hagens M, Slomp CP, Meysman FJR, Seitaj D, Harlay J, Borges AV, Middelburg JJ. 2015. Biogeochemical processes and buffering capacity concurrently affect acidification in a seasonally hypoxic coastal marine basin. Biogeosciences 12:1561–1583.

18. Sulu-Gambari F, Seitaj D, Meysman FJR, Schauer R, Polerecky L, Slomp CP. 2016. Cable bacteria control iron–phosphorus dynamics in sediments of a coastal hypoxic basin. Environ Sci Technol 50(3):1227–1233.

19. Malkin SY, Rao AM, Seitaj D, Vasquez-Cardenas D, Zetsche E-M, Hidalgo-Martinez S, Boschker HTS, Meysman FJR. 2014. Natural occurrence of microbial sulphur oxidation by long-range electron transport in the seafloor. ISME J 8:1843–54.

20. Hofmann AF, Soetaert K, Middelburg JJ, Meysman FJR. 2010. AquaEnv : An aquatic acid–base modelling environment in R. Aquat Geochem 16:507–546.

21. Moore EK, Villanueva L, Hopmans EC, Rijpstra WIC, Mets A, Dedysh SN, Sinninghe Damsté JS. 2015. Abundant trimethylornithine lipids and specific gene sequences are indicative of Planctomycete importance at the oxic/anoxic interface in *Sphagnum*-dominated northern wetlands. Appl Environ Microbiol 81:6333–6344.

22. Quast C, Pruesse E, Yilmaz P, Gerken J, Schweer T, Yarza P, Peplies J, Glöckner FO. 2013. The SILVA ribosomal RNA gene database project: improved data processing and web-based tools. Nucleic Acids Res 41:D590–6.

23. Ludwig W, Strunk O, Westram R, Richter L, Meier H, Yadhukumar, Buchner A, Lai T, Steppi S, Jobb G, Förster W, Brettske I, Gerber S, Ginhart AW, Gross O, Grumann S, Hermann S, Jost R, König A, Liss T, Lüßmann R, May M, Nonhoff B, Reichel B, Strehlow R, Stamatakis A, Stuckmann N, Vilbig A, Lenke M, Ludwig T, Bode A, Schleifer K-H. 2004. ARB: a software environment for sequence data. Nucleic Acids Res 32:1363–71.

24. Jørgensen BB. 1978. Comparison of methods for the quantification of bacterial sulfate reduction in coastal marine-sediments: Measurement with radiotracer techniques. Geomicrobiol J 1:11–27.

25. Guckert JB, Antworth CP, Nichols PD, White DC. 1985. Phospholipid, ester-linked fatty-acid profiles as reproducible assays for changes in prokaryotic community structure of estuarine sediments. FEMS Microbiol Ecol 31:147–158.

26. Boschker HTS, Middelburg JJ. 2002. Stable isotopes and biomarkers in microbial ecology. FEMS Microbiol Ecol 40:85–95.

27. Nanba K, King GM, Dunfield K. 2004. Analysis of facultative lithotroph distribution and diversity on volcanic deposits by use of the large subunit of ribulose 1, 5-bisphosphate carboxylase / oxygenase. Appl Environ Microbiol 70:2245–2253.

28. Nigro LM, King GM. 2007. Disparate distributions of chemolithotrophs containing form IA or IC large subunit genes for ribulose-1,5-bisphosphate carboxylase/oxygenase in intertidal marine and littoral lake sediments. FEMS Microbiol Ecol 60:113–125.

29. Campbell BJ, Stein JL, Cary SC. 2003. Evidence of chemolithoautotrophy in the bacterial community associated with *Alvinella pompejana*, a hydrothermal vent Polychaete. Appl Environ Microbiol 69:5070–5078.

30. Lipsewers YA, Bale NJ, Hopmans EC, Schouten S, Sinninghe Damsté JS, Villanueva L. 2014. Seasonality and depth distribution of the abundance and activity of ammonia oxidizing microorganisms in marine coastal sediments (North Sea). Front Microbiol 5:472. doi:10.3389/fmicb.2014.00472.

31. Tamura K, Peterson D, Peterson N, Stecher G, Nei M, Kumar S. 2011. MEGA5: molecular evolutionary genetics analysis using maximum likelihood, evolutionary distance, and maximum parsimony methods. Mol Biol Evol 28:2731–2739.

32. Saitou N, Nei M. 1987. The neighbor-joining method: a new method for reconstructing phylogenetic trees. Mol Biol Evol 4:406–425.

33. Jukes TH, Cantor CR. 1969. “Evolution of proteins” in *Mammalian protein metabolism*, III. New York Acad. Press - This Week’s Cit Class, 21–132.

34. Zuckerkandl E, Pauling L. 1965. Evolutionary divergence and convergence in proteins, p. 97–166, Evolving Genes and Proteins, *In* Bryson V, Vogel HJ (ed), Academic Press, New York, NY.

35. Bowman JP, McMeekin TA. 2005. Order X. Alteromonadales ord. nov., p 443–491. *In* Brenner D, Krieg N, Staley J, Garrity G (ed), Bergey’s manual of systematic bacteriology US, 2nd ed. vol 2. Springer, New York, NY.

36. Salman V, Amann R, Girnth AC, Polerecky L, Bailey JV., Høgslund S, Jessen G, Pantoja S, Schulz-Vogt HN. 2011. A single-cell sequencing approach to the classification of large, vacuolated sulfur bacteria. Syst Appl Microbiol 34:243–259.

37. Salman V, Bailey J V., Teske A. 2013. Phylogenetic and morphologic complexity of giant sulphur bacteria. Antonie van Leeuwenhoek, Int J Gen Mol Microbiol 104:169–86.

38. Campbell BJ, Engel AS, Porter ML, Takai K. 2006. The versatile ε-proteobacteria: key players in sulphidic habitats. Nat Rev Microbiol 4:458–468.

39. Berg IA. 2011. Ecological aspects of the distribution of different autotrophic CO_2 fixation pathways. Appl Environ Microbiol 77:1925–1936.

40. Hügler M, Sievert SM. 2011. Beyond the Calvin Cycle: Autotrophic Carbon Fixation in the Ocean. Ann Rev Mar Sci 3:261–289.

41. Sorokin DY, Lysenko AM, Mityushina LL, Tourova TP, Jones BE, Rainey FA, Robertson LA, Kuenen GJ. 2001. *Thioalkalimicrobium aerophilum* gen. nov., sp. nov. and *Thioalkalimicrobium sibericum* sp. nov., and *Thioalkalivibrio versutus* gen. nov., sp. nov., *Thioalkalivibrio nitratis* sp. nov. and *Thioalkalivibrio denitrificans* sp. nov., novel obligately alkaliphilic. Int J Syst Evol Microbiol 51:565–580.

42. Takai K, Suzuki M, Nakagawa S, Miyazaki M, Suzuki Y, Inagaki F, Horikoshi K. 2006. *Sulfurimonas paralvinellae* sp. nov., a novel mesophilic, hydrogen- and sulfur-oxidizing chemolithoautotroph within the *Epsilonproteobacteria* isolated from a deep-sea hydrothermal vent polychaete nest, reclassification of *Thiomicrospira denitrificans* as *Sulfurimonas denitrificans comb. nov.* and emended description of the genus *Sulfurimonas*. Int J Syst. Evol Microbiol 56:1725–1733.

43. Labrenz M, Grote J, Mammitzsch K, Boschker HTS, Laue M, Jost G, Glaubitz S, Jürgens K. 2013. *Sulfurimonas gotlandica* sp. nov., a chemoautotrophic and psychrotolerant epsilonproteobacterium isolated from a pelagic redoxcline, and an emended description of the genus *Sulfurimonas*. Int J Syst Evol Microbiol 63:4141–4148.

44. Llobet-Brossa E, Rabus R, Böttcher ME, Könneke M, Finke N, Schramm A, Meyer RL, Grötzschel S, Rosselló-Mora R, Amann R. 2002. Community structure and activity of sulfate-reducing bacteria in an intertidal surface sediment : a multi-method approach. Aquat Microb Ecol 29:211–226.

45. Miyatake T. 2011. Linking microbial community structure to biogeochemical function in coastal marine sediments. PhD Dissertation. University of Amsterdam: Amsterdam.

46. Muyzer G, Stams AJM. 2008. The ecology and biotechnology of sulphate-reducing bacteria. Nat Rev Microbiol 6:441–456.

47. Vestal JR, White DC. 1989. Lipid Analysis in Microbial Ecology. Bioscience 39:535–541.

48. Taylor J, Parkes RJ. 1983. The cellular fatty acids of the sulphate-reducing bacteria, *Desulfobacter* sp., *Desulfobulbus* sp. and *Desulfovibrio desulfuricans*. J Gen Microbiol 129:3303–3309.

49. Edlund A, Nichols PD, Roffey R, White DC. 1985. Extractable and lipopolysaccharide fatty acid and hydroxy acid profiles from *Desulfovibrio* species. J Lipid Res 26:982–988.

50. Nielsen LP, Risgaard-Petersen N, Fossing H, Christensen PB, Sayama M. 2010. Electric currents couple spatially separated biogeochemical processes in marine sediment. Nature 463:1071–1074.

51. Meysman FJR, Risgaard-Petersen N, Malkin SY, Nielsen LP. 2015. The geochemical fingerprint of microbial long-distance electron transport in the seafloor. Geochim Cosmochim Acta 152:122–142.

52. Pfeffer C, Larsen S, Song J, Dong M, Besenbacher F, Meyer RL, Kjeldsen KU, Schreiber L, Gorby YA, El-Naggar MY, Leung KM, Schramm A, Risgaard-Petersen N, Nielsen LP. 2012. Filamentous bacteria transport electrons over centimetre distances. Nature 491:218–221.

53. Schauer R, Risgaard-Petersen N, Kjeldsen KU, Tataru Bjerg JJ, Jørgensen BB, Schramm A, Nielsen LP. 2014. Succession of cable bacteria and electric currents in marine sediment. ISME J 8:1314–1322.

54. Inagaki F, Takai K, Kobayashi H, Nealson K, Horikoshi K. 2003. *Sulfurimonas autotrophica* gen. nov., sp. nov., a novel sulfur-oxidizing ε-proteobacterium isolated from hydrothermal sediments in the Mid-Okinawa Trough. Int J Syst Evol Microbiol 53:1801–1805.

55. Donachie SP, Bowman JP, On SLW, Alam M. 2005. Arcobacter halophilus sp. nov., the first obligate halophile in the genus *Arcobacter*. Int J Syst Evol Microbiol 55:1271–1277.

56. Zhang CL, Huang Z, Cantu J, Pancost RD, Brigmon RL, Lyons TW, Sassen R. 2005. Lipid biomarkers and carbon isotope signatures of a microbial (*Beggiatoa*) mat associated with gas hydrates in the Gulf of Mexico. Appl Environ Microbiol 71:2106–2112.

57. Webster G, Watt LC, Rinna J, Fry JC, Evershed RP, Parkes RJ, Weightman AJ. 2006. A comparison of stable-isotope probing of DNA and phospholipid fatty acids to study prokaryotic functional diversity in sulfate-reducing marine sediment enrichment slurries. Environ Microbiol 8:1575–1589.

58. Finster K, Liesack W, Thamdrup B. 1998. Elemental sulfur and thiosulfate disproportionation by *Desulfocapsa sulfoexigens* sp. nov., a new anaerobic bacterium isolated from marine surface sediment. Appl Environ Microbiol 64:119–125.

59. Böttcher ME, Thamdrup B, Gehre M, Theune A. 2005. $^{34}S/^{32}S$ and $^{18}O/^{16}O$ fractionation during sulfur disproportionation by *Desulfoulfobulbus propionicus*. Geomicrobiol J 22:219–226.

60. Thomsen U, Kristensen E. 1997. Dynamics of sum CO_2 in a surficial sandy marine sediment : the role of chemoautotrophy. Aquat Microb Ecol 12:165–176.

61. Pjevac P, Kamyshny A, Dyksma S, Mußmann M. 2014. Microbial consumption of zero-valence sulfur in marine benthic habitats. Environ Microbiol 16:3416–3430.

62. Mußmann M, Schulz HN, Strotmann B, Kjær T, Nielsen LP, Rosselló-Mora RA, Amann RI, Jørgensen BB. 2003. Phylogeny and distribution of nitrate-storing *Beggiatoa* spp. in coastal marine sediments. Environ Microbiol 5:523–533.

63. Sayama M, Risgaard-Petersen N, Nielsen LP, Fossing H, Christensen PB. 2005. Impact of bacterial NO3− transport on sediment biogeochemistry. Appl Environ Microbiol 71:7575–7577.

64. Hagen KD, Nelson DC. 1996. Organic carbon utilization by obligately and facultatively autotrophic beggiatoa strains in homogeneous and gradient cultures. Appl Environ Microbiol 62:947–953.

65. Bowles MW, Nigro LM, Teske AP, Joye SB. 2012. Denitrification and environmental factors influencing nitrate removal in Guaymas Basin hydrothermally altered sediments. Front Microbiol 3:377. doi:10.3389/fmicb.2012.00377

66. Schulz HN, Jørgensen BB. (2001). Big bacteria. Annu Rev Microbiology 55:105–137

Table 1: Geochemical characterization, chemoautotrophy rates, and quantification of cable bacteria and Beggiatoaceae in the three stations in Lake Grevelingen for spring (March) and summer (August).

Station		°C	Bottom water*		DOU	OPD	SAD	Suboxic zone**	pH signature***	Chemolitho-autotrophy rate	Cable bacteria biovolume	Beggiatoaceae biovolume
			µM O_2	µM NO_3^-	mmol O_2 m^{-2} d^{-1}	mm	mm	mm		mmol C m^{-2} d^{-1}	mm^3 cm^{-2}	mm^3 cm^{-2}
March	1	5	299 (oxic)	28.2	18.2±1.7	1.8±0.04	17.5±0.7	16	e-SOx	3.1±0.5	2.55	0.02
	2	5	301 (oxic)	27.9	15.8±3.1	2.6±0.65	21.3±2.5	19	Nitrate-storing Beggiatoaceae	1.9±0.1	ND	0.11
	3	5	307 (oxic)	27.7	17.1±5.7	2.4±0.4	41.8±8.6	39	e-SOx	1.4±0.3	2.08	0.05
August	1	17	0 (anoxic)	1.7	0	0	0.9±1.1	0.9	Sulfate reduction/ canonical sulfur oxidation	0.2±0.1	0.11	0.001
	2	17	12 (hypoxic)	11.6	0	0	0.6±0	0.6		0.8±0.3	ND	3.24
	3	19	88 (hypoxic)	10.6	13.9±2.1	1.1±0.1	4.2±2.7	3		1.1±0.5	0.003	0.004

DOU: dissolved O_2 uptake; OPD: O_2 penetration depth; SAD: $\sum H_2S$ appearance depth; e-SOx: electrogenic sulfur oxidation; ND: not determined

*Bottom water is classified as anoxic with O_2 concentration below 1 uM and hypoxic below 63 uM.

**The thickness of the suboxic zone is defined as the average SAD minus the average OPD.

***pH signature serves to indicate the sulfur oxidizing mechanism that dominates the porewater chemistry as described by Seitaj et al. (2015)

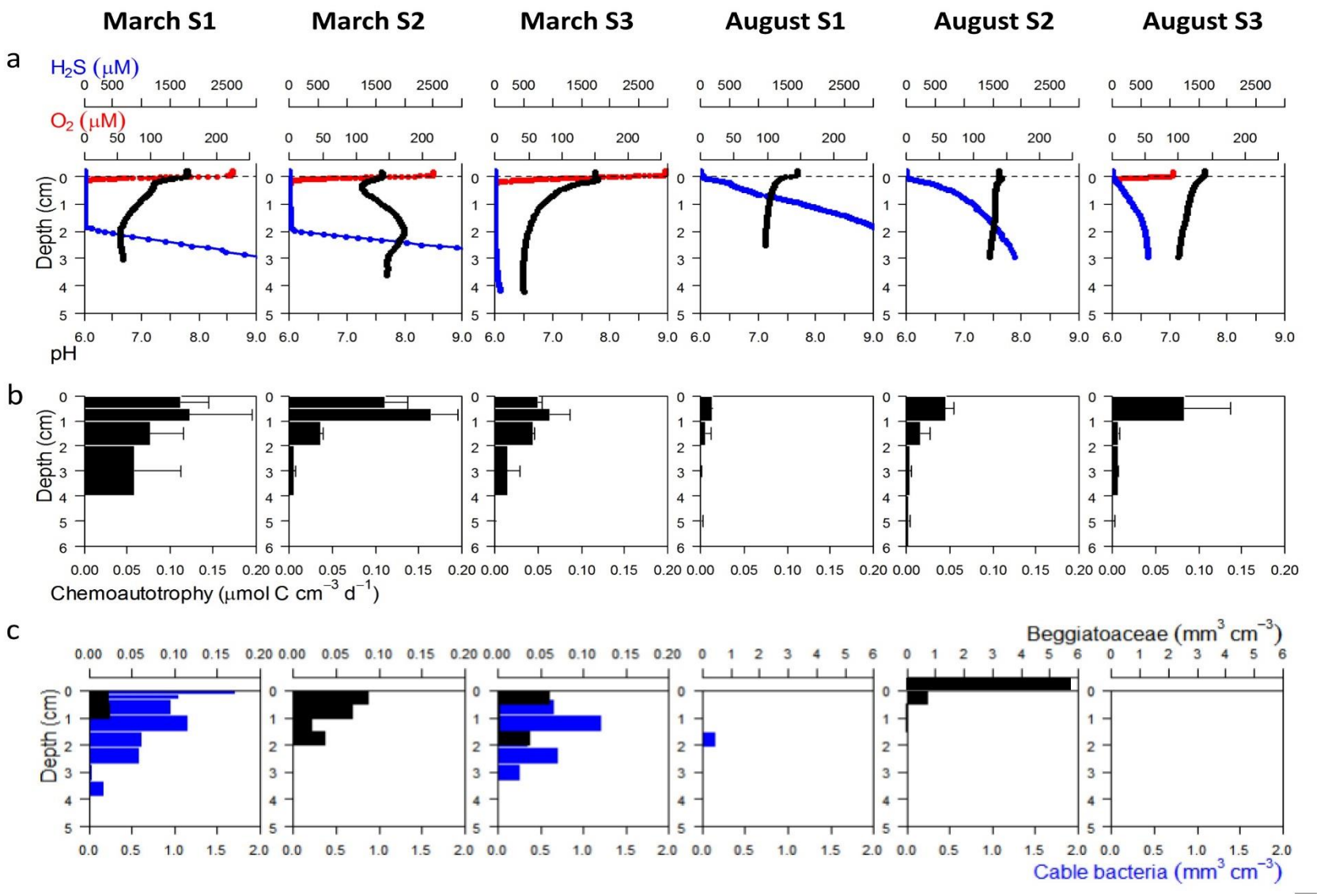

Figure 1: Geochemical fingerprint, (b) chemoautotrophy depth profiles, (c) biovolume of filamentous Beggiatoaceae (black) and cable bacteria (blue) in sediment of Lake Grevelingen for March and August in all three stations (note change in scale for Beggiatoaceae between March and August). S1: station 1 (34 m), S2: station 2 (23 m), S3: station 3 (17 m).

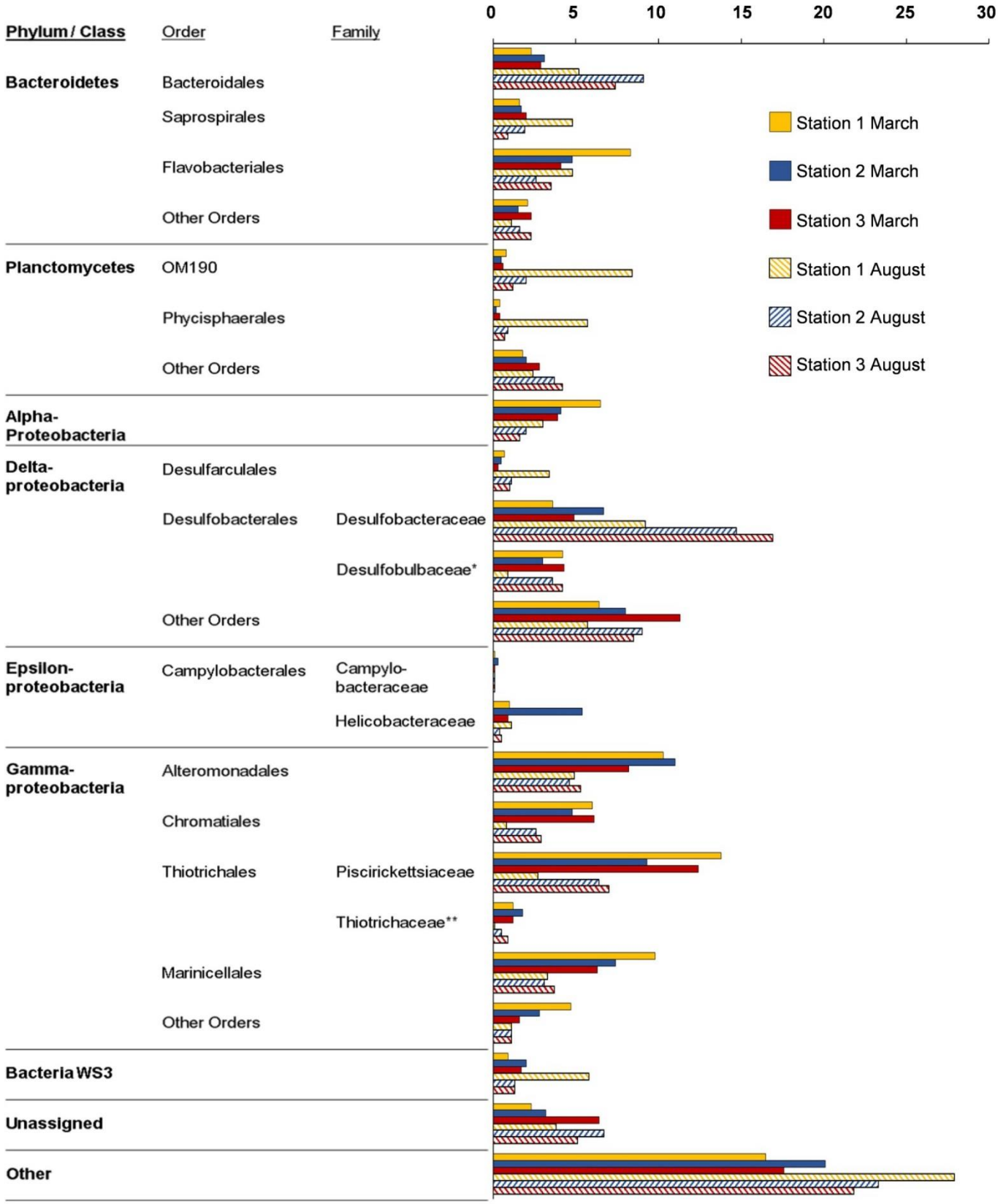

Figure 2: Percentages of total bacterial 16S rRNA gene reads in stations S1 (yellow), S2 (blue) and S3 (red) in March (filled) and August (hatched). Classified bacterial phyla, classes and orders > 3% of the total bacteria reads (in March or August) are reported (exception: family Thiotrichaceae < 3%), *including cable bacteria, **including Beggiatoaceae.

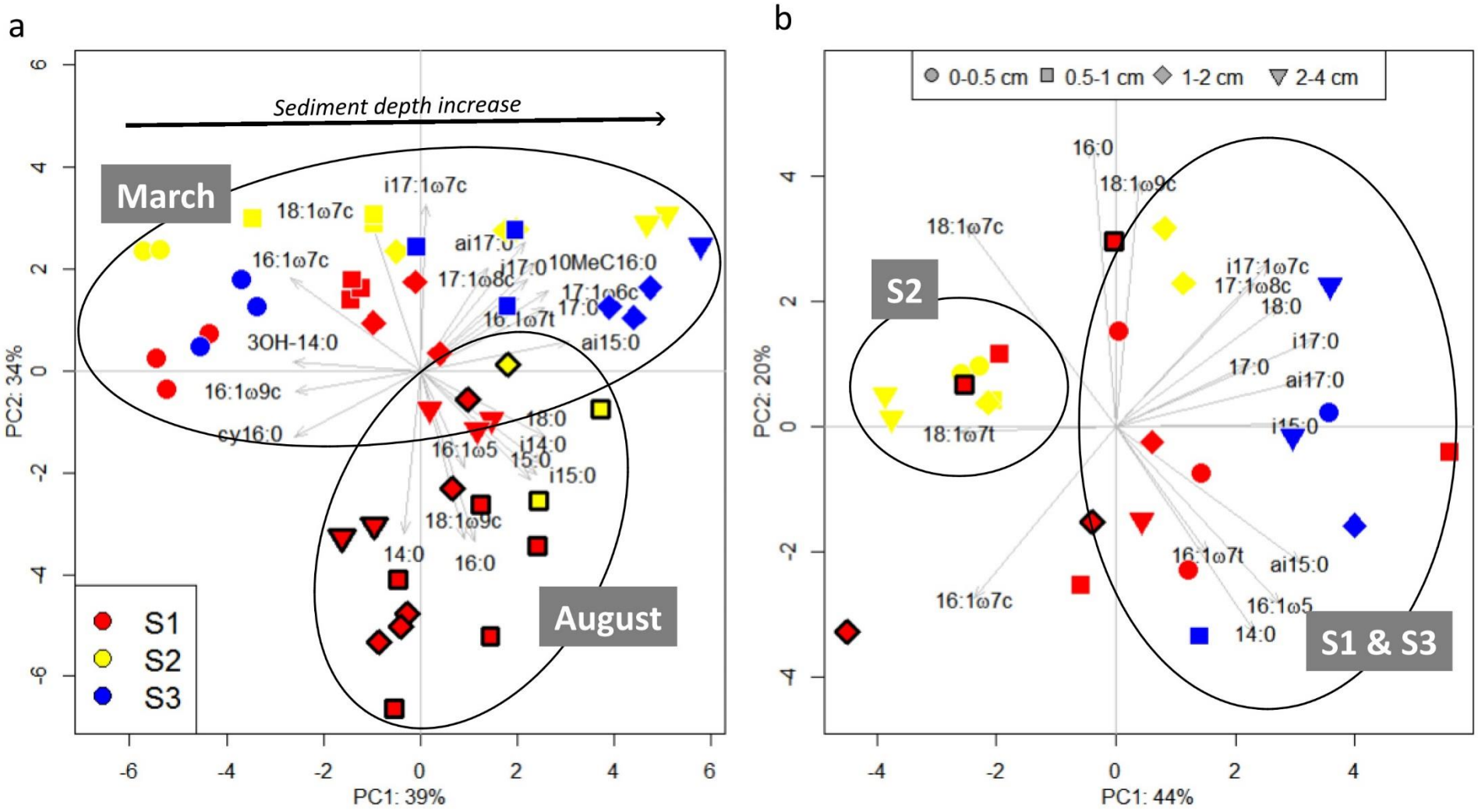

Figure 3: Principal component analysis (PCA) of relative PLFA concentrations (a) and of ^{13}C-incorporation into PLFA (b) in sediments from the three stations in March (no border) and August (black border). The percentage of variability explained by the first two principal components (PC) is indicated on each axis. Red: station S1, Yellow: S2, Blue S3. Symbols indicate sediment depth as seen in plot.

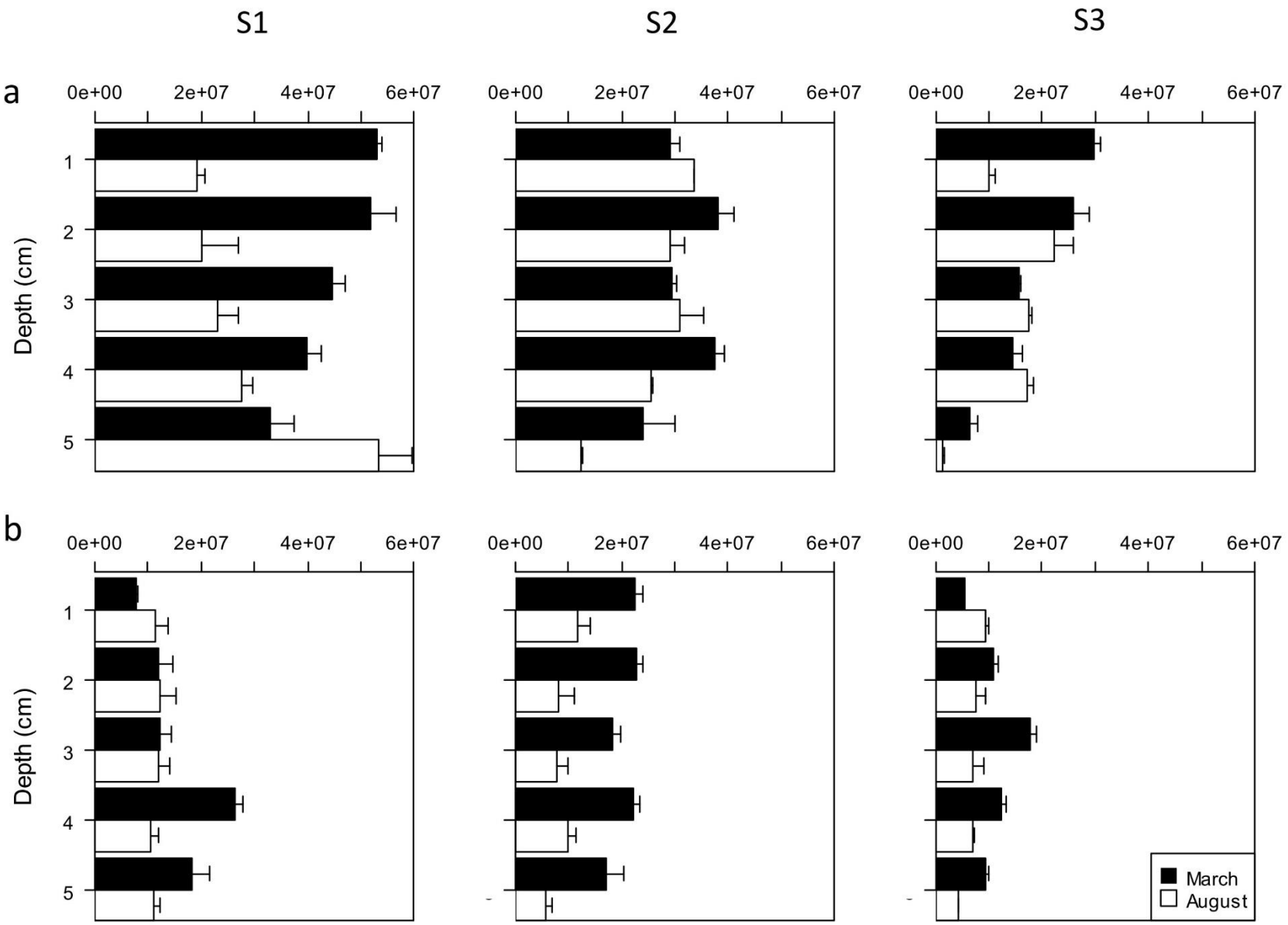

Figure 4: Abundance [copy g^{-1}] of two carbon fixation pathway genes with sediment depth [cm] for S1 (left), S2 (middle) and S3 (right) (a) RuBisCO *cbbL* gene (b) ATP citrate lyase *aclB* gene (black: March, white: August).

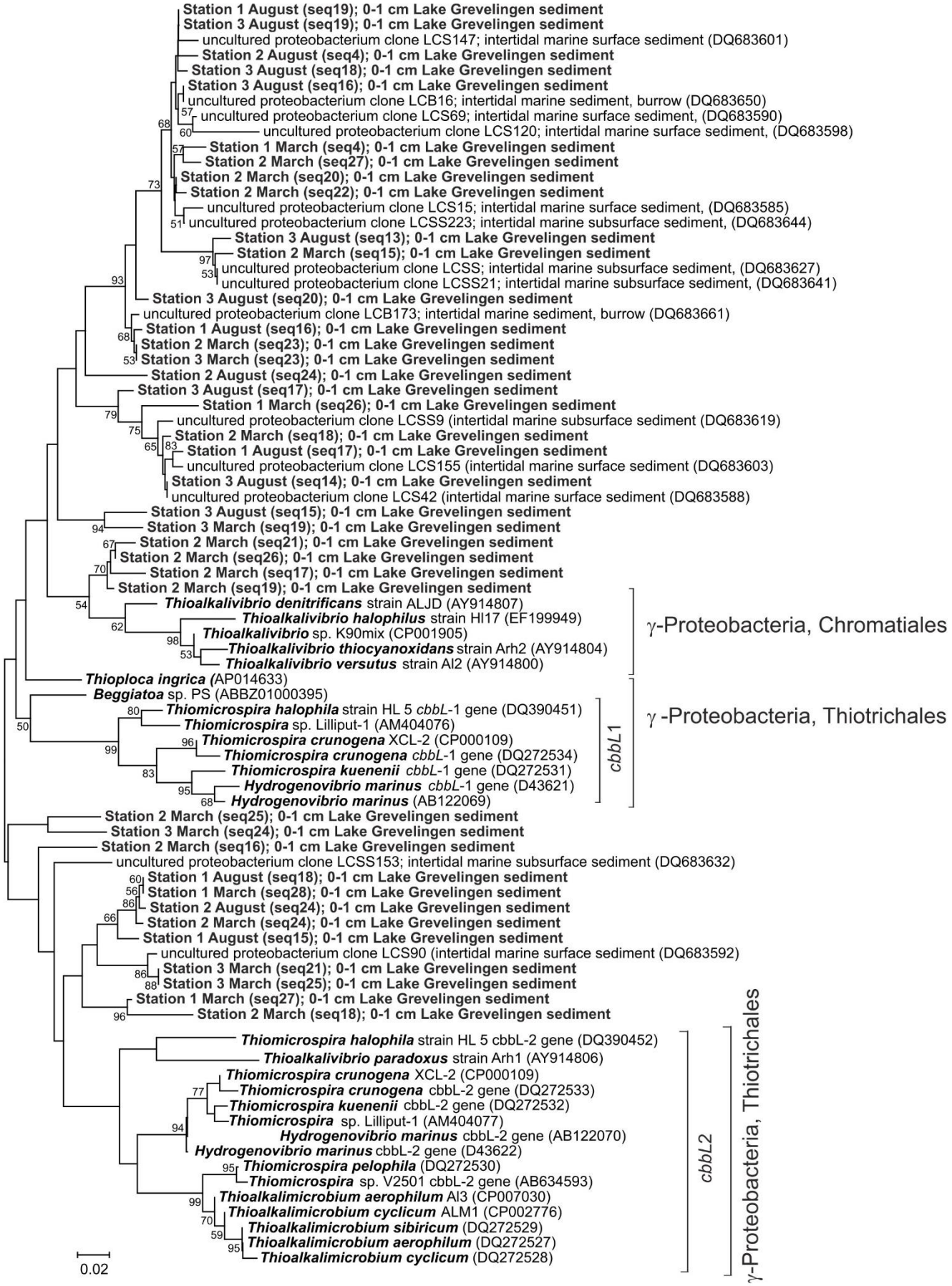

Figure 5A: Phylogenetic tree (amino acid-based) of *cbbL* gene sequences retrieved in this study and closest relatives. Bold: sequences of stations S1, S2 and S3 in March and August and closest known relatives. The scale bar indicates 2% (a) and 5% (b) sequence divergence.

Figure 5B: Phylogenetic tree (amino acid-based) of *aclB* gene sequences retrieved in this study and closest relatives. Bold: sequences of stations S1, S2 and S3 in March and August and closest known relatives. The scale bar indicates 2% (a) and 5% (b) sequence divergence.

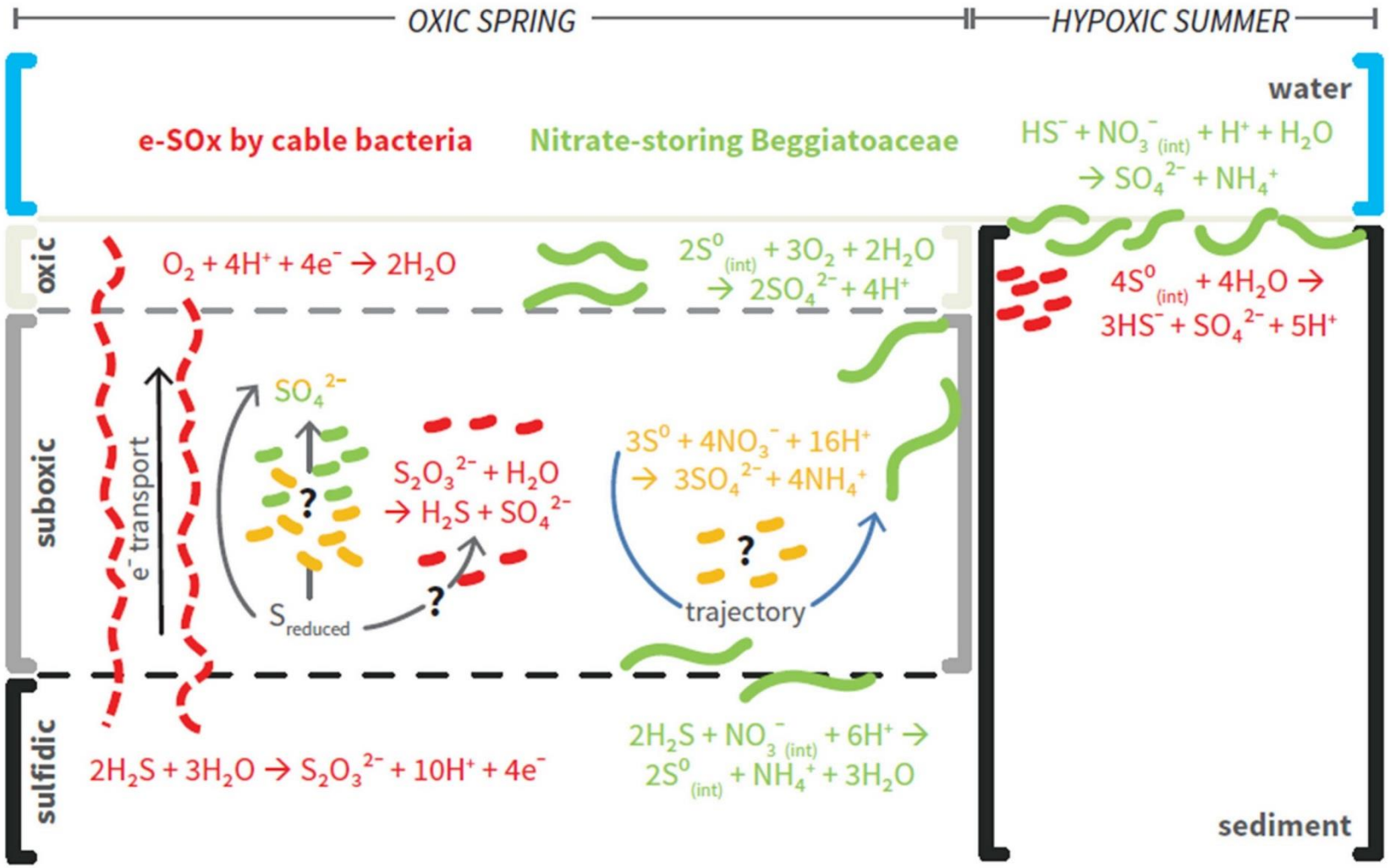

Figure 6: Schematic representation of the main sulfur oxidation mechanisms by chemoautotrophic bacteria under oxic conditions in spring (left) and hypoxic conditions in summer (right) in marine Lake Grevelingen (single-celled and filamentous sulfur-oxidizing bacteria are shown as follows, Epsilonproteobacteria (yellow), Gammaproteobacteria (green), Deltaproteobacteria (red), grey arrows represent possible reoxidation processes by chemoautotrophic bacteria and the color of the reaction indicates the bacterial group involved, blue arrow: trajectory of filamentous Beggiatoaceae (thick green lines) from the surface to the sulfide horizon and back up to the surface, black arrow: long-distance electron transport by cable bacteria (red broken lines).

Supplementary information

Experimental procedures

Aeration of ^{13}C- incubations

To maintain the low oxygen levels found in August at S2 and S3, 30 ml of *in situ* overlying water was removed and cores were closed with rubber stoppers. Headspace was then flushed with N_2 through a needle inserted between the core liner and the rubber stopper without disturbing the water surface. After several minutes, N_2 flushing was stopped and 10 and 35% of the headspace was replaced with air using a syringe for S2 and S3, respectively. No air was added to S1 cores. All cores were gently mixed (0.2 rpm) on a shacking plate to homogenize oxygen concentration in headspace with those in overlying water. At the end of the experiment oxygen saturation in overlying water were verified with oxygen optodes (PreSens Fibox 3 LCD) obtaining anoxic conditions for S1 (0−4% air saturation), hypoxic for S2 (20−26%) and S3 (35−80%).

PLFA nomenclature

The shorthand nomenclature used for phospholipid derived fatty acids is as follows. The number before the colon indicates the number of carbon atoms, while the number after represents the number of double carbon bonds in the fatty acids chain. The position of the initial double bond is then indicated by the last number after the number of carbons from the methyl end (ω). The double bond geometry is designated by cis (c) or trans (t). Methyl branching is described as being in the second carbon iso (i), third carbon anteiso (a) or a number followed by Me is used to indicate the position relative to the carboxyl end (e.g. 10Me16:0). Further details can be found in the literature (Vestal and White, 1989).

PCR 16S rRNA gene amplicon library preparation and analysis

PCR reactions were performed with the universal (Bacteria and Archaea) primers S-D-Arch-0519-a-S-15 (5'-CAG CMG CCG CGG TAA-3') and S-D-Bact-0785-a-A-21 (5'-GAC TAC HVG GGT ATC TAA TCC-3') (Klindworth et al., 2013) adapted for pyrosequencing by the addition of sequencing adapters and multiplex identifier (MID) sequences. To minimize bias three independent PCR reactions were performed containing: 16.3 µL H_2O, 6 µL HF Phusion buffer, 2.4 µL dNTP (25 mM), 1.5 µL forward and reverse primer (10 µM; each containing an unique MID tail), 0.5 µL Phusion Taq and 2 µL DNA (6 ng/µL). The PCR conditions were following: 98ºC, 30 s; 25 × [98ºC, 10 s; 53 ºC, 20 s; 72ºC, 30 s]; 72 ºC, 7 min and 4ºC, 5 min.

The PCR products were loaded on a 1% agarose gel and stained with SYBR® Safe (Life technologies, Netherlands). Bands were excised with a sterile scalpel and purified with Qiaquick Gel Extraction Kit (QIAGEN, Valencia, CA) following the manufacturer's instructions. PCR purified products were quantified with Quant-iT™ PicoGreen® dsDNA Assay Kit (Life Technologies, Netherlands). Equimolar concentrations of the barcoded PCR products were pooled and sequenced on GS FLX Titanium platform (454 Life Sciences) by Macrogen Inc. Korea.

Samples were analyzed using the QIIME pipeline (Caporaso et al., 2010). Raw sequences were demultiplexed and then quality-filtered with a minimum quality score of 25, length between 250−350, and allowing maximum two errors in the barcode sequence. Sequences were then clustered into operational taxonomic units (OTUs, 97% similarity) with UCLUST (Edgar, 2010). Reads were aligned to the Greengenes Core reference alignment (DeSantis et al., 2006) using the PyNAST algorithm (Caporaso et al., 2010). Taxonomy was assigned based on the Greengenes taxonomy and a Greengenes reference database (version 12_10) (McDonald et al., 2012; Werner et al., 2012). Representative OTU sequences assigned to the specific taxonomic groups were extracted through classify.seqs and get.lineage in Mothur (Schloss et al., 2009) by using the greengenes reference and taxonomy files.

In order to determine a more accurate taxonomic classification of the bacterial groups with high percentage of reads and known to contain members with chemolithoautotrophic metabolism, sequence reads of the order Chromatiales and Thiotrichales (Fig. S1, S2), reads of the order Desulfarculales (Fig. S3), the family of Desulfobulbaceae (Fig. S4a) and the genus *Desulfubulbus* (Fig. S4b), reads of the family Desulfobacteraceae (Fig. S5a–c), and additionally reads of the order Campylobacterales (Fig. S6a–d) were extracted from the dataset and added to a phylogenetic tree as described in the Experimental procedures.

Quantification of cable bacteria and Beggiatoaceae

Microscopic identification of cable bacteria was achieved by fluorescence in situ hybridization (FISH), using a Desulfobulbaceae-specific oligonucleotide probe (DSB706; 5′-ACC CGT ATT CCT CCC GAT-3′), according to (Schauer et al., 2014). Cable bacteria biovolume per unit of sediment volume ($mm^3\ cm^{-3}$) was calculated based on measured filament length and diameter. The areal biovolume of cable bacteria ($mm^3\ cm^{-2}$) was obtained by depth integration over all sediment layers analyzed.

The minimum limits of quantification via FISH for single cells were 1.5×10^6 cells cm^{-3}, taken as the FISH count with the negative control probe NON338; a minimum of 1000 DAPI (4,6-diamidino-2-phenylindole) stained cells was

evaluated for this count. The FISH detection limit for cable bacteria was lower than for single cells, and was calculated to be 10 cm filament cm^{-3} (corresponding to <1 filament in 0.1 ml of sediment).

Filamentous Beggiatoaceae were identified via inverted light microscopy (Olympus IM) within 24 h of sediment retrieval. Intact sediment cores were sectioned at 5 mm intervals over the top 4 cm from which subsamples (20−30 mg) were used to count living Beggiatoaceae (Seitaj et al., 2015). The biovolume was determined by measuring length and width of all filaments found in the subsample, following the counting procedure described in (Jørgensen et al., 2010).

Statistical analysis

All statistical analyses were performed using the CRAN: stats package in the open source software R. A two-way ANOVA (aov) was used to test the effect of station, season, and sediment depth on bacterial biomass, chemolithoautotrophic activity, and gene abundances. PLFA concentrations and ^{13}C-incorporation values were expressed as a fraction of the total bacterial biomass and ^{13}C-incorporation (respectively) per sediment sample. These relative PLFA values were first log-transformed (log (x+1)) and subsequently analyzed with Principal Component Analysis (PCA: prcomp) to distinguish different bacterial and chemolithoautotrophic communities in the sediment.

Figure S1−S6: Phylogenetic comparison of bacterial 16S rRNA gene amplicon sequences retrieved in this study, added to a reference tree generated from the SILVA database using the ARB parsimony tool. (red: sequences obtained from stations S1, S2 and S3 in March and August, bold: closest known relatives).

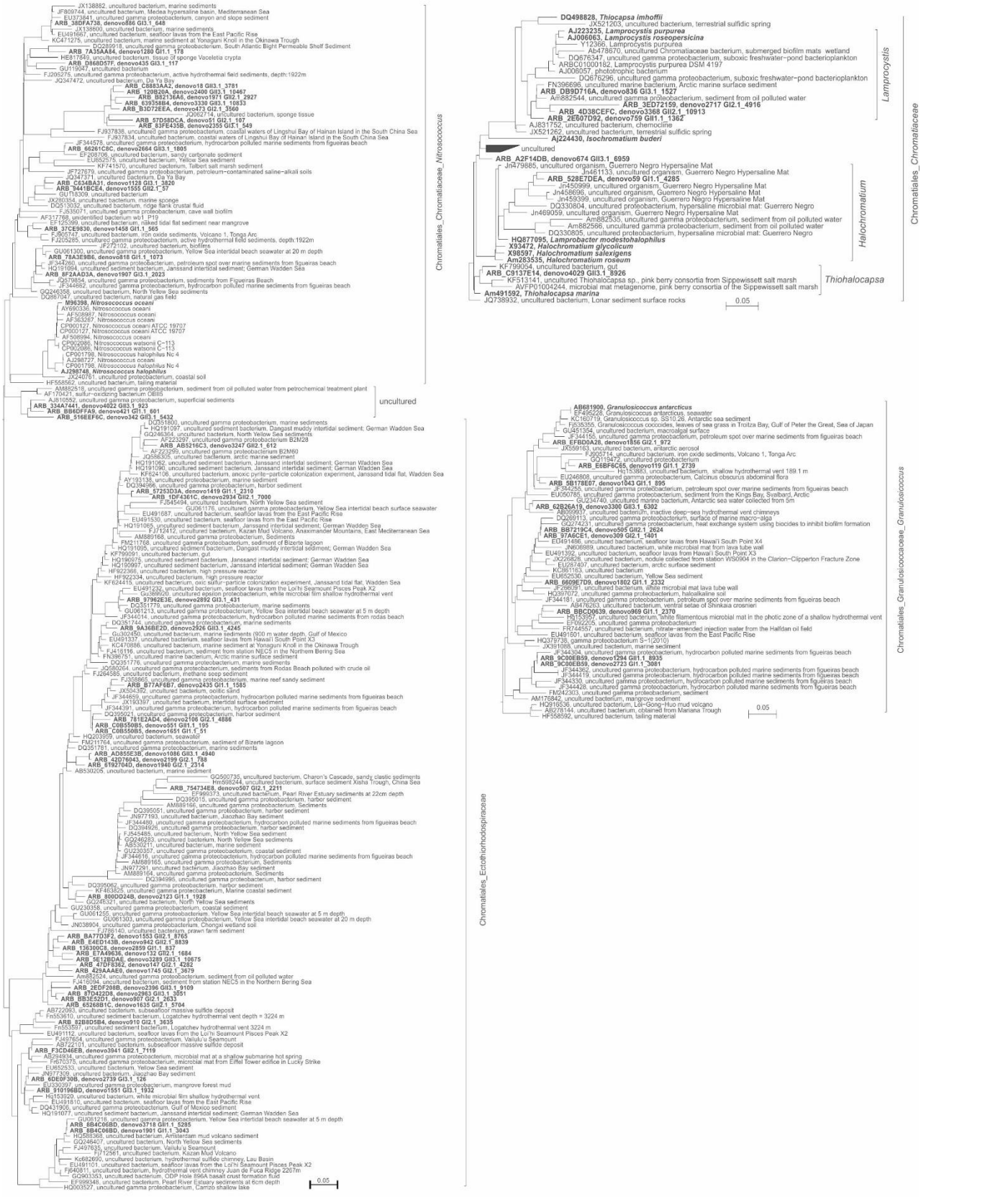

Figure S1: Bacterial 16S rRNA gene amplicon sequences assigned to the class of Gammaproteobacteria, order: Chromatiales.

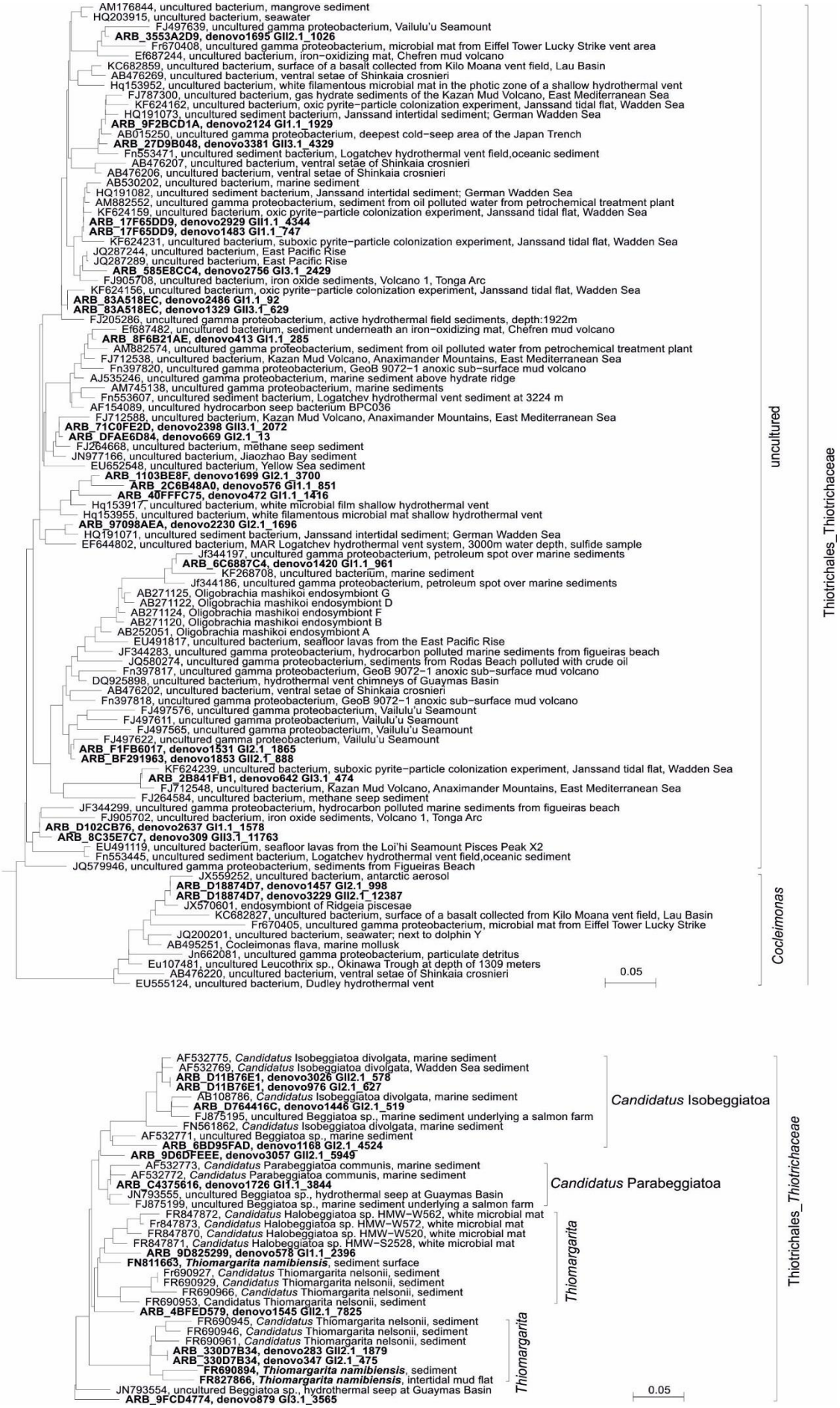

Figure S2: Bacterial 16S rRNA gene amplicon sequences assigned to the class of Gammaproteobacteria, order: Thiotrichales, family: Thiotrichaceae.

Figure S3: Bacterial 16S rRNA gene amplicon sequences assigned to the class of Deltaproteobacteria, order: Desulfarculales.

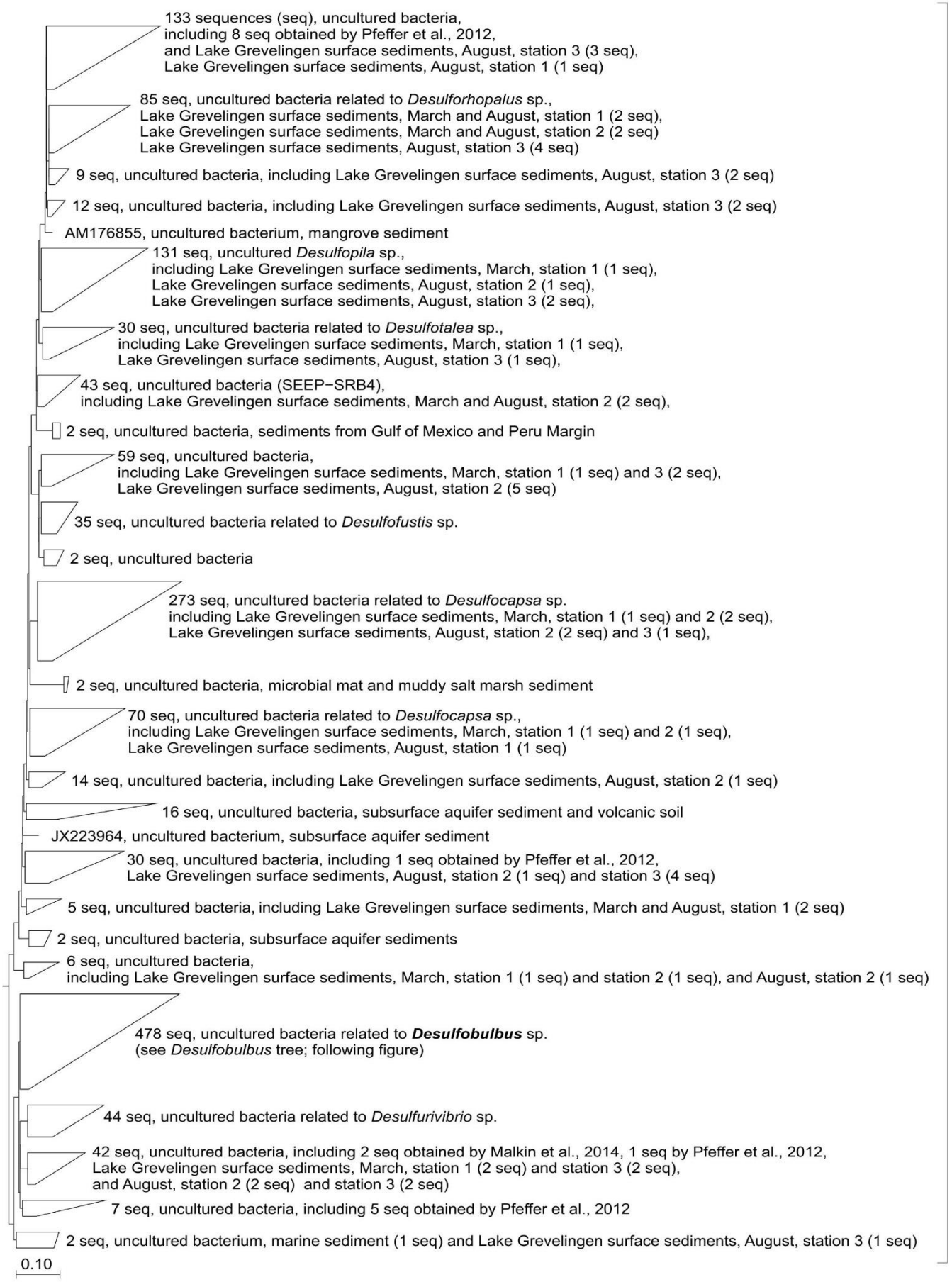

Figure S4a: Bacterial 16S rRNA gene amplicon sequences assigned to the class of Deltaproteobacteria, (a) order: Desulfobacterales, family: Desulfobulbaceae.

Figure S4b: Bacterial 16S rRNA gene amplicon sequences assigned to the class of Deltaproteobacteria, order: Desulfobacterales, family: Desulfubulbaceae.

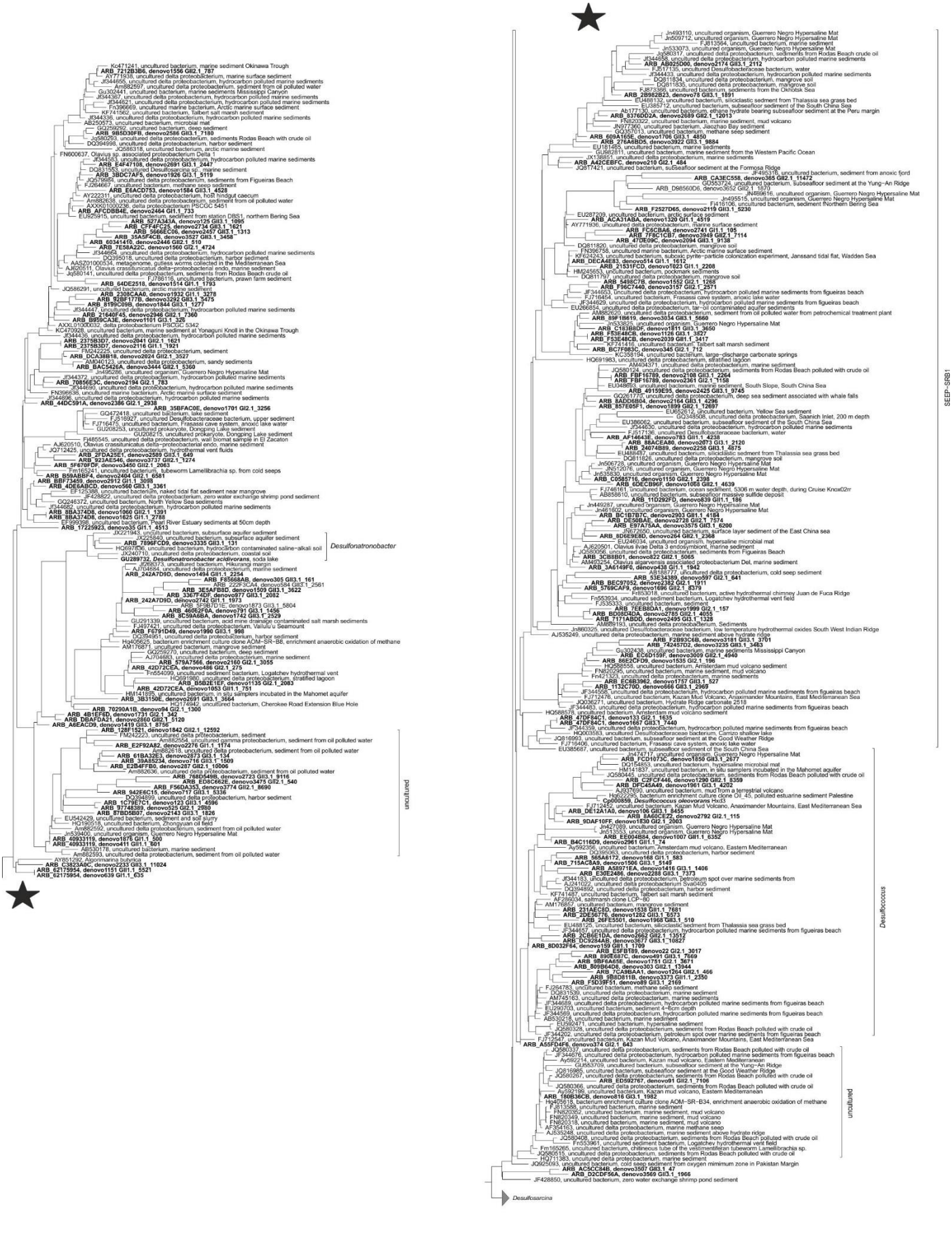

Figure S5a: Bacterial 16S rRNA gene amplicon sequences assigned to in the class of Deltaproteobacteria, order: Desulfobacterales, family: Desulfobacteraceae.

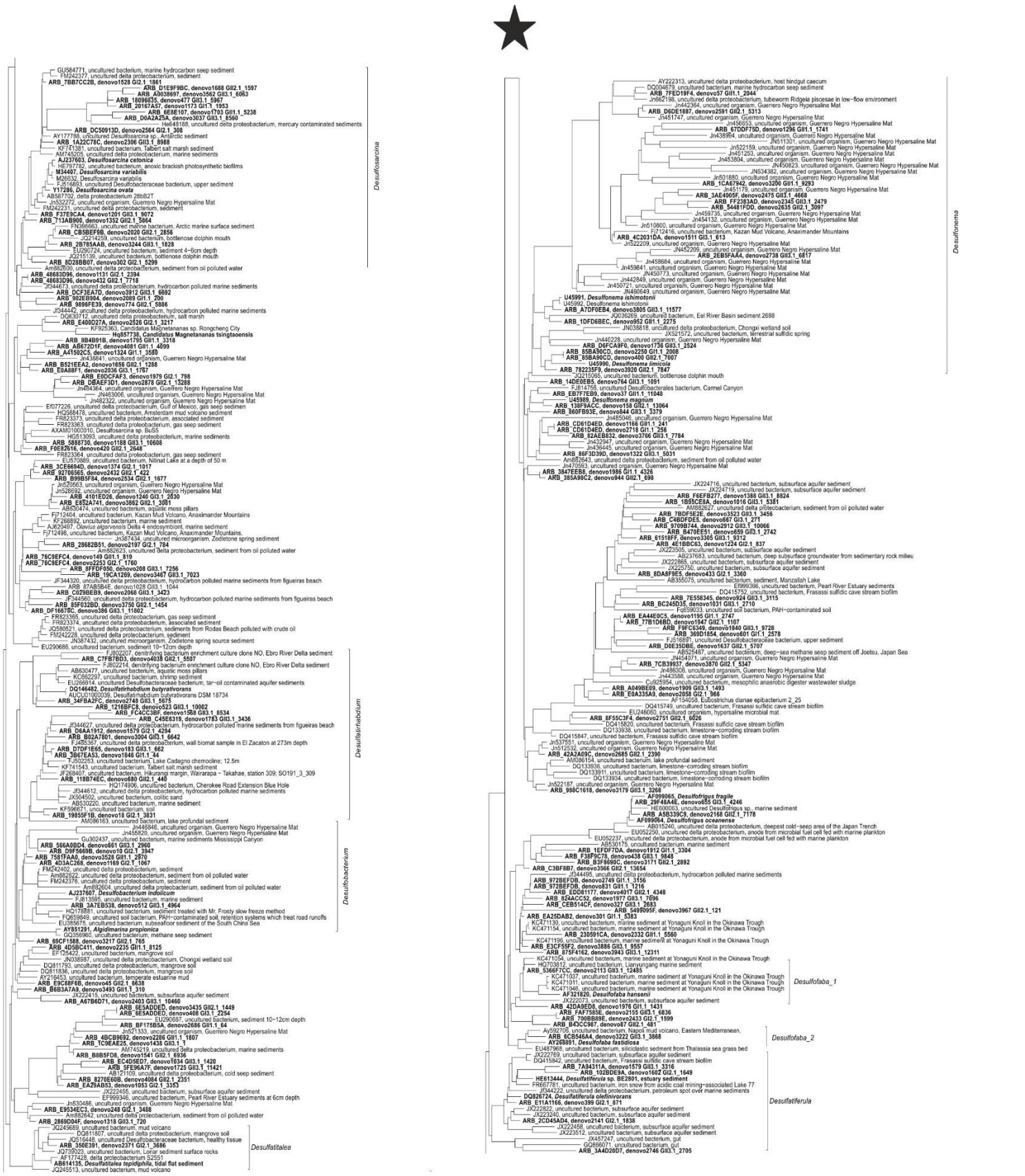

Figure S5b: Bacterial 16S rRNA gene amplicon sequences assigned to in the class of Deltaproteobacteria, order: Desulfobacterales, family: Desulfobacteraceae.

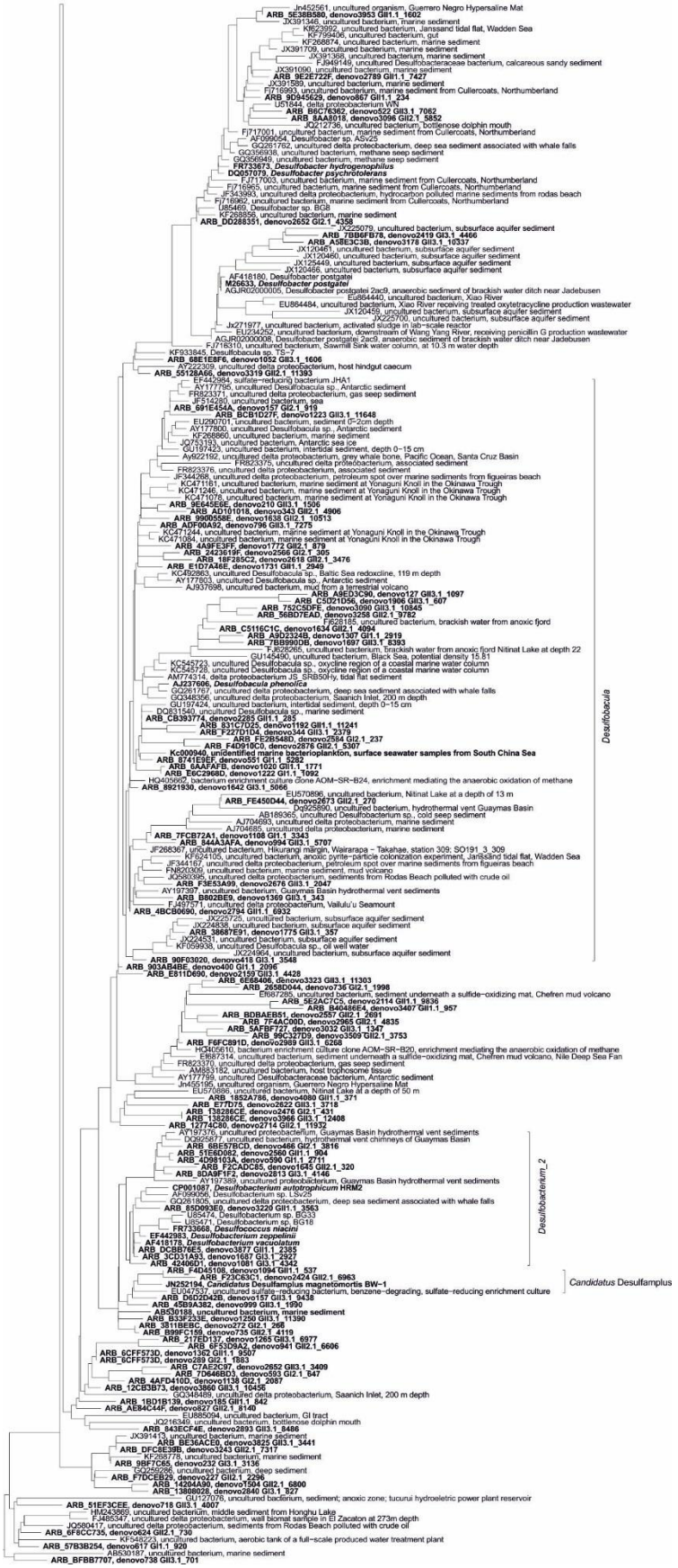

Figure S5c: Bacterial 16S rRNA gene amplicon sequences assigned to in the class of Deltaproteobacteria, order: Desulfobacterales, family: Desulfobacteraceae.

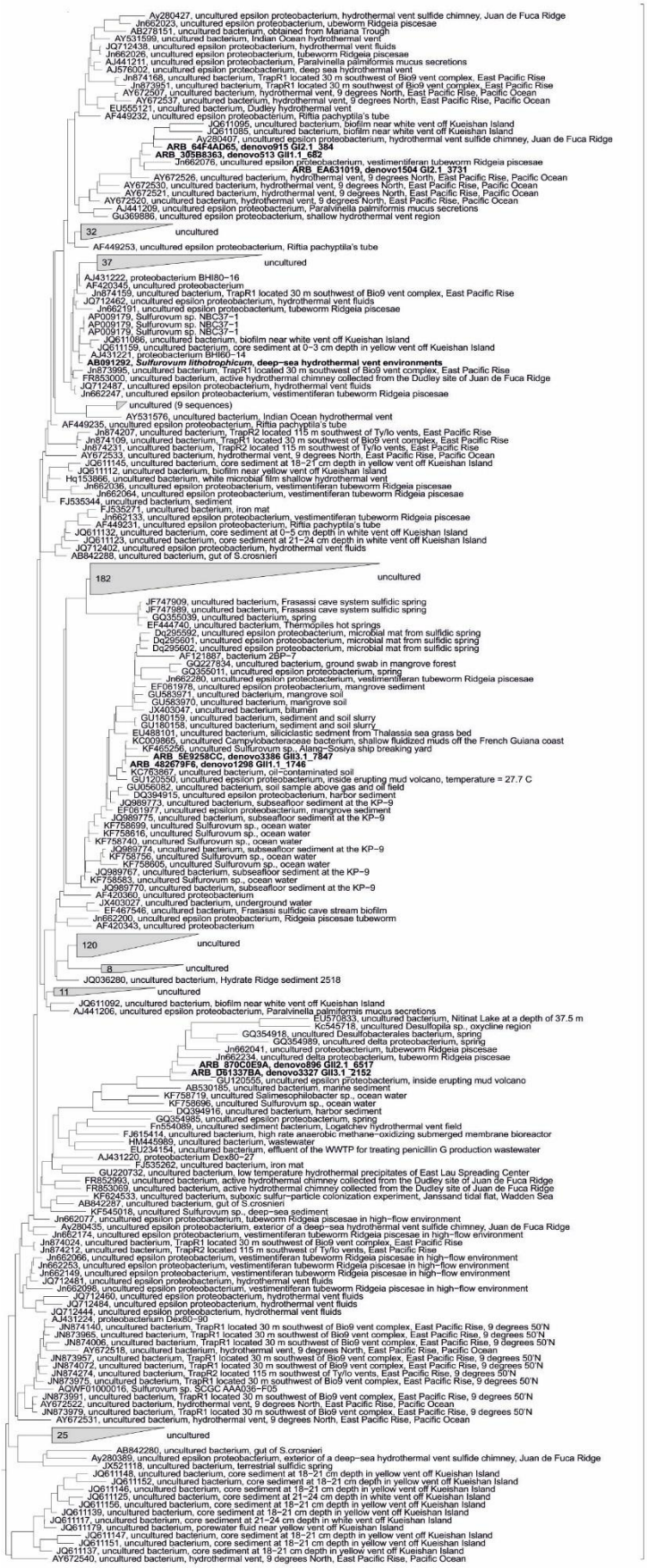

Figure S6a: Bacterial 16S rRNA gene amplicon sequences assigned to the class of Epsilonproteobacteria, order: Campylobacterales, (a) family: Helicobacteraceae, genus: *Sulfurovum*, (b) family: Campylobacteraceae, genus: *Acrobacter*, (c) family: Campylobacteraceae, genus: *Sulfurimonas.*

Figure S6b: Bacterial 16S rRNA gene amplicon sequences assigned to the class of Epsilonproteobacteria, order: Campylobacterales, (a) family: Helicobacteraceae, genus: *Sulfurovum*, (b) family: Campylobacteraceae, genus: *Acrobacter*, (c) family: Campylobacteraceae, genus: *Sulfurimonas.*

Figure S6c: Bacterial 16S rRNA gene amplicon sequences assigned to the class of Epsilonproteobacteria, order: Campylobacterales, (a) family: Helicobacteraceae, genus: *Sulfurovum*, (b) family: Campylobacteraceae, genus: *Acrobacter*, (c) family: Campylobacteraceae, genus: *Sulfurimonas.*

Figure S6d: Bacterial 16S rRNA gene amplicon sequences assigned to the class of Epsilonproteobacteria, order: Campylobacterales, (a) family: Helicobacteraceae, genus: *Sulfurovum*, (b) family: Campylobacteraceae, genus: *Acrobacter*, (c) family: Campylobacteraceae, genus: *Sulfurospirillum.*

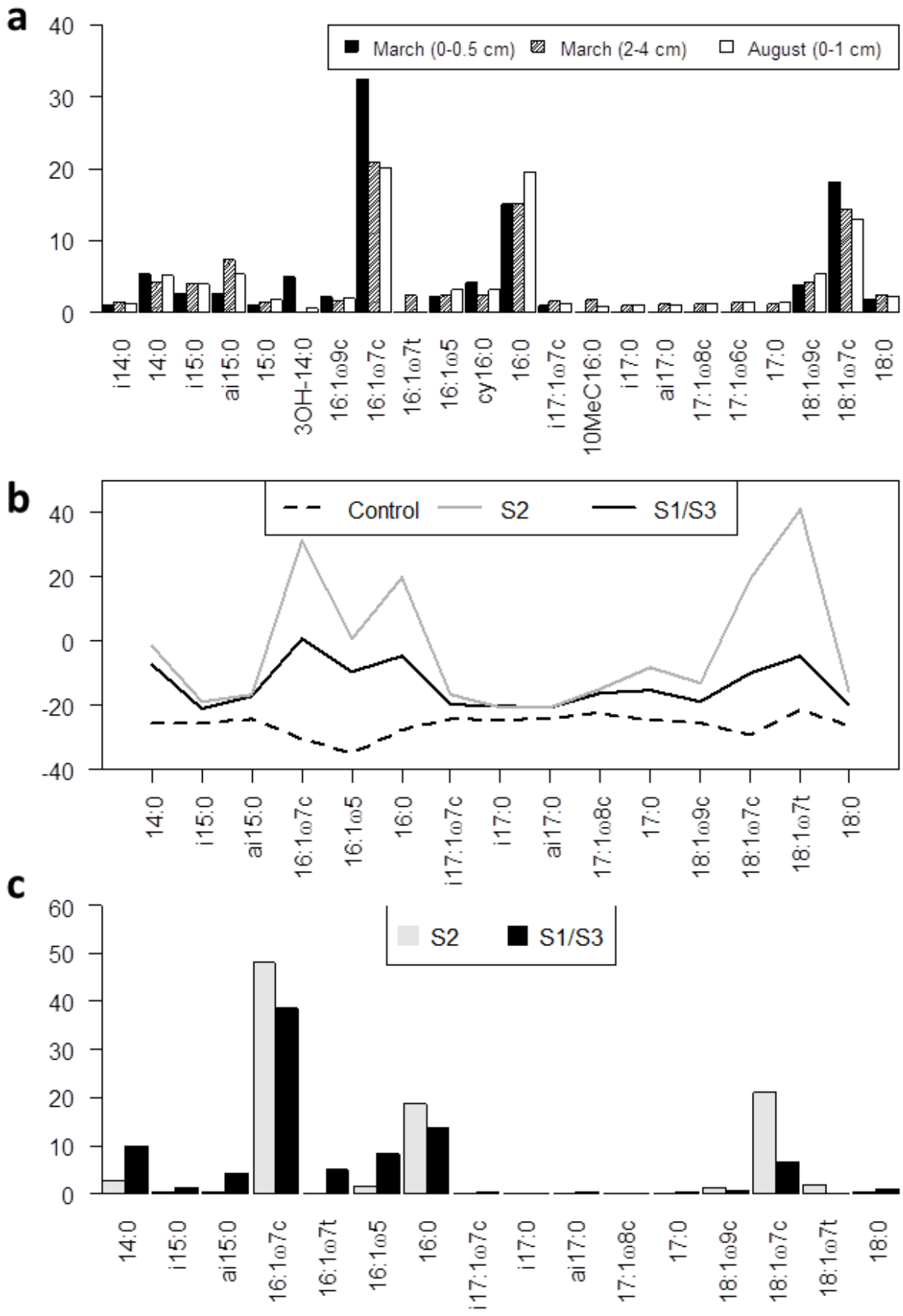

Figure S7: Characteristic PLFA profiles of (a) the average relative concentration of PLFAs for March (0–0.5cm and 2–4 cm) and August (0–1 cm), (b) the average delta ^{13}C values and (c) relative ^{13}C incorporation of PLFAs for S2 and S1/S3 March (0–1 cm).